6335

FTD-TT- 62-1765

405717

405717

25

TRANSLATION

STATISTICAL THEORIES OF STRENGTH AND THEIR APPLICATION TO METALLOCERAMIC MATERIALS (SELECTED PARTS)

Scab-4

FOREIGN TECHNOLOGY DIVISION

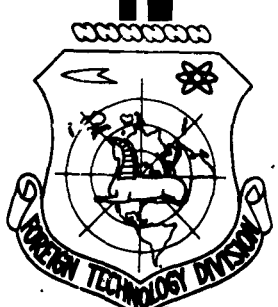

AIR FORCE SYSTEMS COMMAND

WRIGHT-PATTERSON AIR FORCE BASE

OHIO

UNEDITED ROUGH DRAFT TRANSLATION

STATISTICAL THEORIES OF STRENGTH AND THEIR APPLICATION TO METALLOCERAMIC MATERIALS (SELECTED PARTS)

BY: G. S. Pisarenko and V. T. Troshchenko

English Pages: 102

SOURCE: Russian Book, Statistichni Teorii Mitsnosti Ta Ikh Zastosuvannya Do Metalokeramichniki Materialiv, Akademiya Nauk Ukrains'koy RSR, Vidavnitstvo Akademii-Nauk Ukrains'koy RSR, Kiev, 1961, pp. 13-19 and 40-102

PREPARED BY:

TRANSLATION DIVISION
FOREIGN TECHNOLOGY DIVISION
WP-AFB, OHIO.

TABLE OF CONTENTS

Chapter Two

Peculiarities of the Breakdown of Brittle Metalloceramics

1. Some physico-mechanical properties of brittle metaloceramic metarials.

Until recently the use of brittle materials in constructions subjected to the action of force, was very limited. In this connection the number of works dedicated to the research of the strength of materials which brittlely break down, was insignificant, and their main purpose was an over-all study of conditions of brittle breakdown of steels and other alloys, which possess a considerable plastic deformation under normal conditions /1-3, 19, 20/.

Research was also done on strength properties of such brittle materials as glass, quartz /21, 22/, hard alloys for cutting tools /23, 24/ and others.

The picture changed recently, primarily due to the need to produce new materials to work under extremely high temperatures.

It appears that strength and some other properties of common refractory alloys do not answer the requirements of materials used for parts in constructions of the latest engineering methods; tasks looming before constructors can be solved, using such unusual materials as oxides, carbides, silicides, nitrides, borides of high-melting metals, polycrystalline graphite, and others which, by their nature are brittle, but possess certain useful properties which plastic materials do not and cannot have, and which have been used in engineering until very recently.

Some properties of these alloys are given in Table 2.

TABLE 2

ALLOY	Temperature of melting or dissociation T°C	Elasticity module E · 10^{-3} kg/mm^2	Specific gravity g/cm^3	Strength on bending kg/mm^2 (2)
Titanium carbide TiC /8/	3250	3.5	4.93	60
Chromium carbide Cr_3C_2 /4/	1895	--	6.68	--
Tungsten carbide WC /25/	2600	7.14	15.6	35 (3)
Silicon carbide SiC-β /8/	2100 (1)	--	3.21	2.8
Niobium carbide NbC /25/	3500	3.43	7.8	--
Zirconium carbide ZrC /25/,	3530	--	6.8	9.8 (3)
Boron carbide B_4C /25/	2450	--	2.52	30.9
Tantalum carbide TaC /8/	3880	2.91	14.3	--
Aluminum oxide Al_2O_3 /8/	2015	3.78	3.92	26.4 (3)
Beryllium oxide BeO /8/	2550	3.18	2.98	(21?-1050°C)
Magnesium oxide MgO /8/	2800	2.8	3.44	9.80 (3)
Zirconium dioxide ZrO_2 /8/	2600	1.89	5.64	14 (11-1000°C)
Molybdenum silicide $MoSi_2$ /5, 27/	2030	2.76	6.3	25-40
Silicon nitride Si_3N_4 /5/	1900	1.16 ÷ 1.45	3.18 ÷ 3.21	16.0; 14.7 (1200°C)
Graphite /8,26/	3700	0.0914	2.26	295 (1000°C)

1) Converts to SiC -d.

2) Without technology of producing specimens, porosity, dimensions of specimen and other characteristics of strength, can be regarded as orientation figures only.

3) Elongation strength.

The alloys cited in Table 2, which are now of the greatest interest, have the following peculiarities and future uses /5, 8, 25/:

Titanium carbide (T_m = 3250°) has a high melting temperature, high stability, heat resistance *); it is used in hard alloys for cutting tools and in cermets for parts of gas turbines.

Chromium carbide (T_m = 1895°) is used in making wear-resistant parts, and parts of gas turbines.

Tungsten carbide (T_m = 2600°) is used in making hard alloys for cutting tools. High solidity and low tendency to absorption of neutrons provides a future use in atomic power production as a material of heat isolating elements.

Silicon carbide (T_m = 2100°) is used in the production of nozzles and parts of combustion chambers of jet engines, and is a possible material for heat isolating elements of atomic reactors.

Niobium carbide (T_m = 3500°), zirconium carbide (T_m = 3530°) and tantalum carbide (T_m = 3880°) have a high melting temperature, and are regarded as future materials for heat isolating elements of atomic reactors.

Aluminum oxide (T_m = 2015°) has good strength, impact ductility, hardness, it is a satisfactory insulator, stable in various atmospheres and chemical media, strength is maintained up to the temperature of the order of 1100°. Baked aluminum oxide (mineraloceramic) is used as material for cutting instruments.

Boron carbide (T_m = 2450°) represents a future material in the control systems of atomic reactors.

Beryllium oxide (T_m = 2550°) has an extremely high heat conductivity and high strength under high temperatures. Future use in high

temperatures and rapid temperature changes; used in atomic reactors as

*) By heat resistance we understand the property of material to resist acute temperature changes.

retarder of fast neutrons.

Magnesium oxide (T_m = 2800°) is the most widespread refractory material, comparatively inexpensive; high coefficient of thermal expansion; used in temperatures up to 1700°.

Zirconium dioxide (T_m = 2600°) has very low heat conductivity; stable in contact with many metals and oxides, could be a good insulator.

Molybdenum silicide (T_m = 2030°) is used as a covering to protect high melting metals from oxidation (primarily molybdenum) at high temperatures; used in production of heaters for resistance furnaces; the stability of molybdenum silicide against the action of molten metals gives expectation to use it as refractory and material for heat exchangers of atomic boilers.

Silicon nitride (T_m = 1900°) extremely stable to oxides, as well as some molten metals.

Graphite (T = 3700°) is highly fire resistant; stable to many molten metals and other corrosive media; low elasticity module, high heat conductivity and low coefficient of linear expansion provide it with high heat resistance; used in atomic power production at retarder of fast neutrons.

Production of parts from similar materials is usually performed by the powder metallurgy method. As is well known, powder metallurgy, or as it is also called metalloceramics, is a branch of metallurgy which is concerned with production of materials and products from metallic and nonmetallic powders /7 - 9, 28/.

A typical engineering process of powder metallurgy consists of obtaining powder or a mixture of powders, pressing, baking pressed preparations at temperatures lower than the melting temperature of the basic component and final processing (grinding, calibrating, tight pressing, thermal processing, etc.).

Powder metallurgy offers considerable advantages compared with other methods and has become quite widespread in engineering. The advantages of powder metallurgy consist primarily in the fact that it makes it possible to obtain new materials which could not otherwise be obtained. These include porous metal materials, high melting and hard alloys, compositions of metals and nonmetallic materials, for example: graphite-copper, iron-copper and others, compositions of metals which do not mix in liquid state and do not produce hard solutions or intermetallic compositions (iron-lead, tungsten-copper, and others).

Another basic advantage of the powder metallurgy method is the opportunity of mass production of metal parts with minimum labor and no loss of metal in cutting.

Materials and products made by the method of powder metallurgy, can be divided into the following basic groups, depending on the use.

1. High melting metals (tungsten, molybdenum, tantalum etc.) for use in radio engineering and for other special uses.

2. High melting alloys (oxides, carbides, silicides, nitrides, etc.).

3. Cermets which represent a combination of ceramic material (carbides, oxides, etc.) in the form of grains and metal compounds (Ni, Co and others) which cement the ceramic grains into a single whole. These materials are to be used in high temperatures.

4. Hard alloys for cutting tools.

5. Antifriction materials (porous and nonporous).

6. Friction materials.

7. Porous metal-ceramic products (filters, iron for caulking pipe, etc.).

8. Metal[1]oceramic machine building parts (pinions, washers, etc.).

9. Contact materials.

10. Magnetic materials.

11. Electrical engineering materials, etc.

Out of the above metal-ceramic materials, typical brittle materials are high-melting alloys, cermets and hard alloys with a low content of binder; the peculiarities of their breakdown are discussed in this work.

It should be noted that a majority of the materials cited in Table 2 are only beginning to be introduced in practice, and there are numerous difficulties associated primarily with the lack of plasticity in these materials, however, as we have already noted, their advantageous properties - high melting temperature, low specific gravity, high heat resistance and acid resistance etc. make them irreplaceable in solving many problems of modern engineering.

It may yet be possible to achieve some lowering of the brittleness of parts made from these materials while preserving their advantageous properties. This is primarily associated with the use of special binding materials and selection of forms and dimensions of the particles of phase components.

The effect of these factors on plasticity can be observed on cast iron. Thus, common cast iron with laminar graphite is a brittle material, modified cast iron with spherical graphite can have a reserve deformation up to 25%. It is therefore important in many instances not so much to reach a considerable reserve deformation before breakdown, as to have certain phase components in the material which can localize local breakdowns. Examples of such materials are cermets and silico-carbide compositions with graphite, in which there is a combination of the strong carbide carcass with the submissible components /6/.

In Table 3 we cite certain properties of hard alloys and cermets, produced by the method of powder metallurgy.

Among them we will distinguish hard alloys for cutting tools (VK6, VK10, T5K10, T60K6) and cermets for parts of gas turbines, particularly blades (paddles) (K162V, WZ-12a, "Carboloy Cr_3C_2).

Table 3

Material and its Composition	Elasticity module $E \cdot 10^{-3}$ kg/mm^2	Specific gravity g/cm^3	Strength limit for bend kg/mm^2	Impact strength kg/mm^2
VK6 /7/ (94% WC, 6% Co)	4.8 - 6.0	14.80	120	0.25
VK10 /7/ (90% WC, 10% Co)	4.8 - 6.0	14.40	135	0.20 /17/
T5K10 /7/ (85% WC, 9% Co, 6% TiC)	--	12.3 - 13.2	115	--
T60K6 /7/ (34% WC; 60% TiC; 6% Co)	--	6.5 - 7.0	75	--
K162V /29/ (62% TiC; 8%(Ta,Nb,Ti)C; 25% Ni, 5% Mo)	4.16	5.65	--	0.35
WZ-12a /30/ (75% TiC; 15% Ni; 5% Co, 5% Cr)	4.18	6.00	120 - 130	0.38
"Carboloy Cr_3C_2" grade 608 /8/ (83% Cr_3C_2; 2% WC, 15% Ni)	--	7.00	--	--

The creation of these materials contributed to considerable progress in the respective branches of engineering and industry. The use of hard alloys in machine building made it possible to increase the speed of cutting metals from 300 to 3,000/m/sec, and also made it possible to process such materials as glass, porcelain, stone, etc., which would not be processed before by any means.

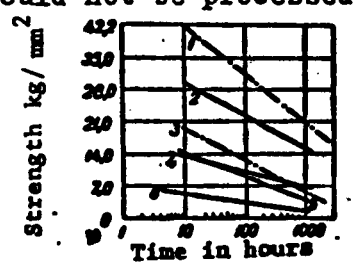

Fig. 9. Durable strength of cermet on a base of TiC (K162V) and special heat-resistant alloy Co-Cr-Ni:

1 - K162V, t = 872°, taking into account tightness; 2 - K162V, t = 872°; 3 - K162V, t = 982°, taking into account tightness; 4 - K162V, t = 982°; 5 - alloy Co-Cr-Ni, t = 872°; 6 - alloy Co-Cr-Ni, t = 982°.

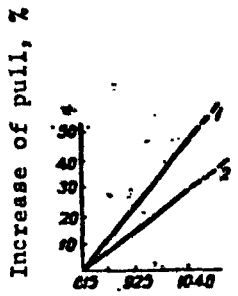

Fig. 10. Effect on pull of motor by temperature of gas at turbine input:

1 - turbo-jet motor; 2 - turbo-prop motor.

The use of cermets in gas turbine building makes it possible to increase the operating parameters of turbines considerably. This is clearly illustreated in Figs. 9 /8/ and 10 /29/. In Fig. 9 we cite data of durable strength of ceramo-metellic metarial K162V and heat-resistant alloy Co-Cr-Ni, which show that durable strength of cermet is much higher than that of alloy Co-Cr-Ni. The difference becomes even greater if we consider the specific gravity of these materials.*)

We can see from the curves in Fig. 10 the manner in which the pull of jet and turbo-prop engines increases with the increase of the temperature of gas at the turbine input. Simultaneously the specific expenditure of fuel decreases.

The use of new materials for individual parts, construction joints and whole constructions, destined to operate at very high

*) In some instances(for example, in the case of working blades /paddles/ of turbines) it is not difficult to obtain high strength of material as the high ratio of strength to specific gravity of the material. Accordingly, with similar parts, all other conditions being equal, materials with low specific gravity are the most promising.

temperatures and great loads, required a whole gamut of research of the strength properties of heat-resistant materials like these.

The data obtained as a result of this research, along with the results of previous investigations show that the following rules governing in general the breakdown of brittle metaloceramic materials can be observed:

1. The basic difference between the technical and theoretical strength, if the latter is calculated on the basis of the atomic theory of composition of the material.

2. The essential dispersion of results of tests for strength.

3. Considerable differences between strength in compression and elongation and the most essential effect of maximum elongation stresses on strength.

4. Decrease of characteristics of strength with increase of the dimensions of specimens.

5. Essential effect of the form of load on characteristics of strength (bend, pure bend, elongation).

6. Increase of strength in the interval of high temperatures compared with strength at normal temperature, and some others.

Chapter Three

Statistical Theories of Brittle Strength

1. General Considerations

An analysis of the laws governing the breakdown of brittle metal-ceramic materials[1], cited above, indicates that we cannot obtain sufficiently founded dependencies for the calculating of strength of these materials, if we do not consider their following properties: a) breakdown is caused by normal elongation stress (effect of abutting and pressing tensions on strength is insignificant); b) the cause of breakdown is micro-cracks (and other similar defects), which are fortuitously distributed over the entire volume of the material.*)

The effect on strength of fortuitously distributed micro-defects over the volume of the material is taken into account by statistical theories of brittle strength. A majority of these theories is based on the following assumptions for each class of material considered:

1. The cause of breakdown is a micro-crack (or other defect).

2. Micro-cracks do not change their characteristics during the process of loading until the very beginning of breakdown.

3. One micro-crack of critical dimension suffices to cause a breakdown of the entire specimen regardless of its dimensions.

*) In the case of materials with an obviously preponderant effect on strength of surface defects (glass, quartz) we do not calculate the volume of the material, but its surface. This case is not considered here.

4. A certain critical stress of elongation corresponds to each material which, when reached, is the beginning of breakdown.

5. A certain function of distribution of critical stress along micro-cracks corresponds to each material.

This function of distribution is graphically shown in Fig. 21, where the magnitude of the limit of strength is plotted along the axis of the abscissae, which the specimen would possess, if the given defect were the cause of breakdown, and along the axis of the ordinates - its corresponding solidity of probability p (σ).

The aggregate of assumptions cited above, is sometimes jointly referred to as the hypothesis of "the weak link."

Founded on this hypothesis are the theories of Kontorova and Frenkel' /62, 65/, Weibull /47/, Fisher and Hollomon /66/ and some others /67/.

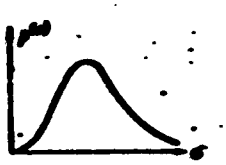

Fig. 21. Distribution of critical stresses along micro-cracks of solid bodies.

The problem, formulated above, is analogous to the problem of mathematical statistics on the distribution of least values in the excerption of dimension n, taken from the general total according to the law of distribution P(x) /11, 14, 67/. Utilizing the results of mathematical statistics, we can write the following expressions for the distribution of the extreme terms of the variation series.

For the first term:

$$\varphi(x_1) = np(x)[1 - P(x)]^{n-1} \qquad (72)$$

or, as has been shown (52), (53)

$$\Omega(x_1) = 1 - /1 - P(x)/^n$$

for the nth term

$$\Omega(x_n) = /P(x)/^n.$$

The contents of these equations are as follows: if, from the general total, which has distribution p(x), we take a large number of excerptions of volume n and for each excerption we erect a variation series, then the least and greatest value of this variation series will have a distribution according to Formulas (52, 53).

The most probable value of the least magnitude (mode) can be found from the equation

$$\frac{d[\omega(x_1)]}{dx} = 0 \qquad (73)$$

or

$$p^2(x^*)(n-1) = [p'(x^*)][1-P(x^*)]. \qquad (74)$$

where x^* is the most probable value of the least magnitude in the excerption of volume n.

Depending on the form of distribution of p(x) the connection between x^* and the volume of excerption n can be different. Some data on this problem are cited in Table 14 /67, 14/.

Table 14

Law of Distribution	Function of distribution of probabilities	Most probable value of least magnitude in excerption
Distribution according to the law of equal probability	$p(x) = \frac{1}{b-a}$; $a \leqslant x \leqslant b$ $p(x) = 0$ in every other place	
Cauchy distribution	$p(x) = \frac{1}{\pi} \frac{\lambda}{\lambda^2 + (x-\mu)^2}$	$\mu = \frac{\lambda a}{2\pi}$
Laplace distribution	$p(x) = \frac{1}{2\lambda} \exp\left[-\frac{(x-\mu)}{\lambda}\right]$	$\mu = \lambda \lg \frac{a}{2}$

Normal distribution	$p(x) = \frac{1}{\Delta\sqrt{2\pi}} \exp\left[-\frac{(x-a)^2}{2\Delta^2}\right]$	$a - \Delta(2\lg n)^{1/2} + A\frac{\lg\lg n + \lg 4\pi}{2(2\lg n)^{1/2}}$
Weibull distribution	$p(x) = amx^{m-1}\exp[-ax^m]$ $x>0;\ a>0;\ m>1$ $P(x) = 1-\exp[-ax^m]$	$\frac{1}{[an]^{1/m}}\left(1-\frac{1}{m}\right)^{1/m}$

For the case of brittle strength, purely mathematical concepts can be interpreted as follows:

$$p(x) = \frac{d/P(x)/}{dx}$$

as a function of distribution of critical tensions for micro-cracks;

$$p(\sigma) = \frac{d/P(\sigma)/}{d};$$

n - as the number of micro-cracks in the specimen, whose volume is V(N); x_1 as the strength of a single specimen of volume $V(\sigma')$; x^* - as the most probable value of brittle strength of specimen of volume $V(\sigma^*)$.

Thus, the equation from which we can determine σ^* will be quite analogous to equation (74); it is actually used by all authors who investigated the problem of brittle breakdown from the position of the "weak link."

The differences in results obtained can be explained by the different form of function $p(\sigma')$ and different simplifications which were assumed in solving this equation (74).

In this case the physical picture is fairly clear: the greater the dimensions of the specimen, the greater the probability of encountering in it a dangerous defect, and the lower is strength; out of two forms of load the one is more dangerous in which the volume of the ma-

terial is in the zone of maximum tensions. From this viewpoint the mean elongation strength should be lower than of pure bend, and in

pure bend - lower than in a bend by concentrated power, and so on.

In considering the strength of material by taking into account the statistical factor, it is advisable to introduce the concept of nonuniformity of material, which is determined by the dispersion of the curve of distribution of critical tensions along the microcracks. The greater this dispersion, the more nonuniform the material, and vice versa.

A conformity of experimental data to formulas of the statistical theories of strength based on the hypothesis of the "weak link" can only be expected when breakdown occurs brittlely and in the process of loading there are no essential changes in the picture of distribution of tension along the individual micro-volumens of the material.

Nevertheless in many instances, for example, in the case of materials which have a certain plasticity, cyclical application of loads, etc., this hypothesis does not correspond to the real picture of breakdown, although even in these cases the nonuniformity of properties and tension of individual micro-volumes can have a real effect on the process of breakdown.

These instances are considered in the statistical theories of strength of Volkov /69-72/, Afanas'yev /74/ Freudenthal /75/ and others.

2. Existing Statistical Theories of Strength

The Theory of T. Kontorova and Ya. Frenkel' /65/

Relying on the hypothesis of the "weak link," the authors found the following expression of the probability of encountering a specimen whose brittle strength lies in the interval $\sigma_1; \sigma_1 + d\sigma$:

$$\omega(\sigma_1)\,d\sigma = \overline{N}Vp(\sigma_1)|l(\sigma_1)|^{N-1} \qquad (75)$$

where $\bar{N}$ is the mean number of microdefects in the material within 1 cm^3; V is the operational volume of the material; $p(\sigma)$ is the function of distribution;

$$I(\sigma_1) = \int_{\sigma_1}^{\infty} p(\sigma)\, d\sigma.$$

Assuming the function of distribution according to the Gauss law, which the authors write in the form

$$p(\sigma) = Ce^{-\alpha(\sigma-\sigma_0)^2}, \tag{76}$$

where

$$C = \frac{1}{\sqrt{2\pi(\sigma-\sigma_0)^2}}; \quad \alpha = \frac{1}{2(\sigma-\sigma_0)^2};$$

is the strength corresponding to the most frequently encountered defect, we can find

$$\omega(\sigma_1)\, d\sigma = C\bar{N}Ve^{-\alpha(\Delta\sigma)^2}[I(\Delta\sigma)]^{\bar{N}V-1}\, d\sigma, \tag{77}$$

where

$$\sigma_0 - \sigma_1 = \Delta\sigma; \quad \sigma - \sigma_0 = y;$$

$$I(\Delta\sigma) = C\int_{-\Delta\sigma}^{\infty} e^{-\alpha y^2} dy.$$

For the case $\sigma_1' < \sigma_1$, i.e. large specimens,

$$\omega(\sigma_1)\, d\sigma \simeq C\bar{N}Ve^{-\alpha(\Delta\sigma)^2}\left[1 - \frac{e^{-\alpha(\Delta\sigma)^2}}{2\alpha\Delta\sigma}\right]^{\bar{N}V}. \tag{78}$$

hence it follows that the probability of encountering a specimen with strength σ_1' diminishes with the increase of volume.

Differentiating expression (75) along σ_1', Kontorova and Frenkel' found such an equation which should be satisfied by the most probable value of the strength of the specimen with volume V,

$$\frac{\partial p(\sigma^*)}{\partial\sigma^*} - \frac{\bar{N}V[p(\sigma^*)]^2}{I(\sigma^*)} = 0, \tag{79}$$

where

$$p(\sigma^*) = Ce^{-\alpha(\sigma-\sigma_0)^2};$$

$$I(\sigma^*) = \int_{\sigma^*}^{\infty} p(\sigma)\, d\sigma.$$

The equation obtained is analogous to (74), cited above.

Using (79), Kontorova and Frenkel, by means of certain approximations, found for large values of V the following expression for the a posteriori value of brittle strength of the specimen upon elongation:

$$\sigma^* = \sigma_0 - \sqrt{A \lg V + B}, \qquad (80)$$

where

$$A = \frac{1}{\alpha};$$

$$B = \frac{1}{\alpha} \lg \frac{N}{2\sqrt{\pi}}.$$

In the case of small volumes, Kontorova and Timoshenko (62/ showed that the a posteriori value of brittle strength is

$$\sigma^* \cong a + \frac{b}{V}. \qquad (81)$$

where

$$a = \sigma_0 - \frac{1}{2\sqrt{\alpha}};$$

$$b = \frac{\sqrt{\pi}}{2\sqrt{\alpha} N}.$$

The function obtained (81) is very close to the formula which was proposed by Aleksandrov and Zhurkov /21/ on the basis of the analysis of the results of testing for break thin glass and quartz thread.

Kontorova and Timoshenko /62/ also tried to spread the proposed theory to the case of nonuniform state of stress. For specimens of large dimensions in the case of pure bend, they obtained

$$\sigma^*_{p.b.} \cong \sigma_0 - \sqrt{A \lg V + B_{p.b.}}. \qquad (82)$$

where σ_0 and A are the same magnitudes as in the case of elongation;

$$B_{p.b.} = \frac{1}{\alpha} \lg \frac{N}{2\sqrt{\pi}\, \alpha \sigma_0}.$$

In the case of twisting

$$\sigma^*_{tw.} \cong \sigma_0 - \sqrt{A \lg V + B_{tw.}}; \qquad (83)$$

where

$$\theta_{tw.} = \frac{1}{a} \lg \frac{2N}{\sqrt{2\pi}a}.$$

The formulas obtained on the basis of this theory, contain three experimental constants of material (α, N, σ_1) whose calculation is difficult.

The basic formula of the theory of Kontorova and Frenkel' (80) is not correct in all instances. Particularly, it is not applicable to very large values of V. In this case σ^* can be less than zero. It is also inapplicable to the case of small V, when σ^* can be an imaginary magnitude. This is explained by the fact that, first of all, the normal law accepted for the distribution of defects provides a certain probability of negative values of the strength of defects, and hence also of negative values of the strength of specimens.

The second inapplicability is associated with the fact that in deriving the ultimate formulas the volume of the specimen (V) was assumed to be large.

The Weibull Theory /47/

The basic magnitude with which Weibull operates is the probability P of brittle breakdown of the specimen during elongation tension which exceeds σ.

If P_0 is the probability of breakdown of a unit of volume of the material, then the probability of breakdown of the specimen with volume V can be found from equation*

$$(1-P_0)^V = 1-P. \tag{84}$$

The expression obtained can be written in the form

$$V \ln(1-P_0) = \ln(1-P). \tag{85}$$

*) In this case we use the precepts of thetheory of probability with reference to the fact that the probability of simultaneous occurrence of several independent events equals the sum total of the probabilities of these events.

Then Weibull assumes

$$B = -\ln(1-P), \tag{86}$$

where he calls B the chance of breakdown.

Assuming that the material is solid, and also assuming the properties of the material to be such that the probability of the start of breakdown at any point, considered from the microscopic viewpoint, is equal, Weibull assumes

$$dB = -\ln(1-P_0)\,dV. \tag{87}$$

Inasmuch as $\ln(1-P_0)$ is a function only of σ and it is negative, he writes:

$$dB = n(\sigma)\,dV. \tag{88}$$

Then in the case of random distribution of stresses along the cross-section, the chance of breakdown is determined according to the formula

$$B = \int n(\sigma)\,dV; \tag{89}$$

the probability of breakdown according to Formula (86) will be in the form

$$P = 1 - e^{-B} = 1 - e^{-\int n(\sigma)\,dV}. \tag{90}$$

The formula obtained is the basic formula of the Weibull theory.

The mean value of brittle strength is determined according to the formula

$$\sigma^0 = \int_{-\infty}^{\infty} \sigma\,dP, \tag{91}$$

whence, considering (90),

$$\sigma^0 = -\int_{-\infty}^{\infty} \sigma\,d\left(e^{-\int n(\sigma)\,dV}\right) =$$

$$= -\left[\sigma e^{-\int n(\sigma)\,dV}\right]_{-\infty}^{\infty} + \int_{-\infty}^{\infty} e^{-\int n(\sigma)\,dV}\,d\sigma.$$

Since the first term of this equation equals zero, therefore

$$\sigma^* = \int_0^\infty \sigma e^{-\int n(\sigma) dV} \cdot \tag{92}$$

Function $n(\sigma)$ is assumed by Weibull in the form

$$n(\sigma) = \left(\frac{\sigma}{\sigma_0}\right)^m. \tag{93}$$

If it is assumed that the strength of the specimen cannot be lower than a certain value, Weibull proposes to assume function $n(\sigma)$ in the form

$$n(\sigma) = \left(\frac{\sigma - \sigma_1}{\sigma_0}\right)^m. \tag{94}$$

Insufficient argumentation of the selection of functions $n(\sigma)$ is the weakest spot of the entire Weibull theory.

With a uniform state of tension, if we consider (93), Formula (90) will assume the form

$$P = 1 - e^{-V\left(\frac{\sigma}{\sigma_0}\right)^m};$$
$$B = V\left(\frac{\sigma}{\sigma_0}\right)^m. \tag{95}$$

It should be noted that Formula (95) can be interpreted from the position of the "weak link" hypothesis as an integral function of the distribution of the most dangerous defects in a specimen of volume V. The distribution of critical tension along microdefects, on the analysis of which are founded similar statistical theories of brittle strength, should correspond to Equation (52).

The expression for the mean strength will be determined by the following formula

$$\sigma^* = \frac{I_m \sigma_0}{\sqrt[m]{V}}, \tag{96}$$

where

$$I_m = \int_0^\infty e^{-z^m} dz;$$

$$z = \frac{\sigma}{\sigma_0}$$

σ_0 is the constant of material which equals the stress giving the unit of volume of the material a probability of breakdown 0.63; m is the coefficient of uniformity of material. Substituting x for z ($z = x^{1/m}$), we will get $I_m = \Gamma(1 + 1/m)$.

Magnitude I_m depends only on m; its value at different m are as follows:

m	1	2	3	4	8	16	∞
I_m	1.00	0.886	0.896	0.908	0.940	0.965	1.00

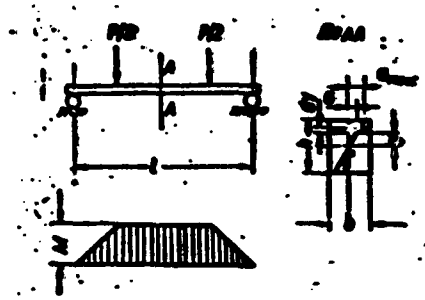

Diagram of the bending moment

Fig. 22. Diagram of pure bending of a rod of rectangular cross-section.

The nonuniformity of the state of tension in the Weibull theory can be calculated by finding the corresponding chance of breakdown according to the formulas

$$B = \int_V s(\sigma)\,dV;$$

$$s(\sigma) = \left(\frac{\sigma}{\sigma_0}\right)^m.$$

Uited below are the results for the basic tests of brittle materials for strength.

Pure bending of rod of rectangular cross-section (Fig.22)

$$\sigma = \sigma_{max}\frac{y}{h};\quad \sigma_{max} = \frac{M}{W};\quad dV = b_1\,dx;$$

$$B = \int_V \left(\frac{\sigma}{\sigma_0}\right)^m dV = bl_1 \left(\frac{\sigma_{max}}{\sigma_0}\right)^m \frac{1}{h^m} \int_0^h y^m dy;$$

$$B = \frac{V}{2(m+1)} \left(\frac{\sigma}{\sigma_0}\right)^m. \qquad (97)$$

Comparing (97) with Formula (95) we will write:

$$\sigma^{\circ}_{p.b.} = \frac{(2m+2)^{1/m}\sigma_0}{V^{1/m}} I_m. \qquad (98)$$

2. Bending of rod of rectangular cross-section by concentrated force (Fig. 23): $\sigma = \sigma_{b.} \frac{2x}{l} y/h;\ dV = bdxdy;$

$$B = \left(\frac{\sigma_{max}}{\sigma_0}\right)^m \frac{2^m}{l^m} \cdot \frac{1}{h^m} b2 \int_0^{l/2} x^m dx \int_0^h y^m dy; \qquad (99)$$

$$B = \left(\frac{\sigma_{max}}{\sigma_0}\right)^m \frac{V}{2(m+1)^2};$$

$$\sigma^{\circ}_{b.} = \frac{2^{1/m}(m+1)^{2/m}\sigma_0}{V^{1/m}} I_m. \qquad (100)$$

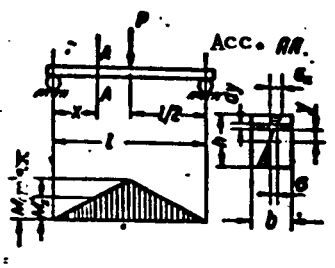

Diagram of bending moment

Fig. 23. Diagram of bending by concentrated force of rod of rectangular cross-section.

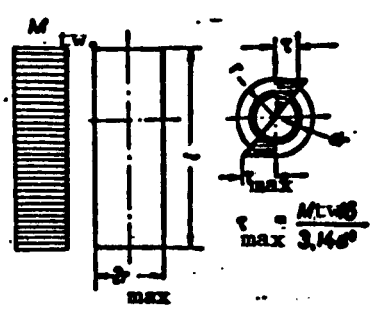

Fig. 24. Diagram of twisting round rod,

where $\tau_{max} = \frac{16\,M_{tw.}}{3{,}14\,d^3}$.

3. Twisting of round rod (Fig. 24).

$$\sigma = \tau; \quad \sigma = \sigma_{max}\frac{r}{r_{max}}; \quad dV = 2\pi r l dr;$$

$$B = \left(\frac{\sigma_{max}}{\sigma_0}\right)^m \frac{r^{2\pi}}{r^m} \int_0^{r_{max}} r^{m+1} dr; \tag{101}$$

$$B = \left(\frac{\sigma_{max}}{\sigma_0}\right)^m \frac{2V}{m+2};$$

$$\sigma_{tw.} = \left(\frac{m+2}{2}\right)^{1/m} \frac{\sigma_0 l_m}{V^{1/m}}. \tag{102}$$

4. Elongation of specimen with cross-section which changes according to the law $F = F_{min} + ay^2$ see infra (Fig.29, VI). This form of specimen is often used in testing metal[1]ceramic materials for elongation. The calculation formula will be in the form

$$\sigma = \frac{\sigma_0}{(2kb_{min}^k)^{1/m}} l_m \tag{103}$$

where σ is the stress in the minimum cross-section of the specimen; h is the height of the specimen; b is the width of the cross-section of the specimen which changes according to the law

$$b = b_{min} + \frac{a}{k} y^k;$$

$$l = \int_0^{\frac{l_{op.}}{2}} \left(b_{min} + \frac{a}{k} y^k\right)^{-m-2} dy.$$

The operational volume of the specimen can be determined by the formula

$$V = 2\int_0^{\frac{l_{op.}}{2}} (F_{min} + ay^k)\, dy. \tag{104}$$

$$V = F_{min} l_{op.} + \frac{a}{12} l_{op.}^3 \tag{105}$$

For specimen VI (Fig.29) b_{min} = 5.5 mm, $\frac{l_{op}}{2}$ = 21 mm, b_{max} = 9.8 mm, R = 105 mm; at h = 4.3mm, V = 1250 mm^3; at h = 5.95 mm, V = 1730 mm^3.

Magnitude I depends on the geometry of the specimen and parameter m. We will cite the values of I for specimen VI (Fig.29) depending on m:

m	2	3	4	5	6	7
I	3.133	0.914	0.208	0.0443	$9.07 \cdot 10^{-3}$	$1.81 \cdot 10^{-3}$
m	8	9	10	11	12	
I	$3.58 \cdot 10^{-4}$	$6.98 \cdot 10^{-5}$	$1.35 \cdot 10^{-5}$	$2.59 \cdot 10^{-6}$	$4.50 \cdot 10^{-7}$	

Comparing the results obtained, we can see that with an identical volume of material under stress brittle strength will differ and the difference will be greater the smaller the value of the coefficient of uniformity of material

$$\sigma : \sigma_{tw.} : \sigma_{p.b.} : \sigma_{b.} = 1 : \left(\frac{m+2}{2}\right)^{1/m} : (2m+2)^{1/m} : 2^{1/m}(m+1)^{2/m}; \qquad /50B/$$

with m = 3

$$\sigma : \sigma_{tw.} : \sigma_{p.b.} : \sigma_{b.} = 1 : 1{,}35 : 2 : 3{,}1. \qquad /50C/$$

The physical argument of the dependencies obtained by Weibull was given in the work of Chechulin /68/ where it is shown that using the basic equation (79) of the theory of Kontorova and Frenkel' and assuming the distribution of defects in the form of the Pearson function of the third grade, it can be proved that the Weibull formula (96) is a special case of a more accurate solution of Equation (79).

The Pearson Function of the third grade has the following form:

$$p(\sigma) = L\sigma^m e^{-\alpha\sigma}, \qquad (106)$$

where L is the normalizing coefficient; m is a constant which determines dispersion; α is a constant which is determined by dispersion and mode. It can be shown that $\alpha = \frac{m}{\sigma_i}$, where σ_i is the a priori most probable local strength (mode).

From the condition of normalizing

$$\int_0^\infty p(\sigma)\,d\sigma = 1$$
$$L = \left(\frac{m}{\sigma_a}\right)^{m+1}\frac{1}{m!} \qquad (107)$$

In the case of a fractional magnitude

$$L = \left(\frac{m}{\sigma_a}\right)^{m+1}\frac{1}{\Gamma(m+1)} \qquad (108)$$

After substitution the Pearson function of disrtibution of the third grade will have the form:

$$p(\sigma) = L\sigma^m e^{-m\frac{\sigma}{\sigma_a}}. \qquad (109)$$

For substitution into Equation (79) we find the value of the integer

$$\int_0^\infty p(\sigma)\,d\sigma = L\int_0^\infty \sigma^m e^{-m\frac{\sigma}{\sigma_a}}\,d\sigma = 1 - L\int_0^\sigma \sigma^m e^{-m\frac{\sigma}{\sigma_a}}\,d\sigma \qquad (110)$$

For the case where m is a whole number, integrating by integrants, Chechulin finds

$$L\int_0^\sigma \sigma^m e^{-m\frac{\sigma}{\sigma_a}}\,d\sigma = -L\left(\frac{\sigma_a}{m}\right)^{m+1} e^{-m\frac{\sigma}{\sigma_a}} m^m\left[\left(\frac{\sigma}{\sigma_a}\right)^m + \right.$$
$$+\frac{m}{m}\left(\frac{\sigma}{\sigma_a}\right)^{m-1} + \frac{m(m-1)}{m^2}\left(\frac{\sigma}{\sigma_a}\right)^{m-2} + \dots$$
$$\left. + \frac{m(m-1)(m-2)\dots 3\cdot 2\cdot 1}{m^{m-1}}\left(\frac{\sigma}{\sigma_a}\right) + \frac{m!}{m^m}\right] + 1. \qquad (111)$$

Marking the polynomial relative to $\left(\frac{\sigma}{\sigma_a}\right)$ in square brackets of the equation by Φ, we can write

$$\int_0^\infty p(\sigma)\,d\sigma = L\left(\frac{\sigma_a}{m}\right)^{m+1} m^m \Phi e^{-m\frac{\sigma}{\sigma_a}}. \qquad (112)$$

Substituting the found functions into Equation (19), we will get

$$Lm\sigma^{m-1}e^{-m\frac{\sigma}{\sigma_a}}\left(1-\frac{\sigma}{\sigma_a}\right) =$$
$$= \frac{NV(L\sigma^m e^{-m\frac{\sigma}{\sigma_a}})^2}{L\left(\frac{\sigma_a}{m}\right)^{m+1} m^m \Phi^2 e^{-m\frac{\sigma}{\sigma_a}}}; \qquad (113)$$

after reductions, the equation will be in the form

$$\left(1-\frac{\sigma^*}{\sigma_u}\right)\Phi^* = \overline{NV}\left(\frac{\sigma^*}{\sigma_u}\right)^{m+1}. \qquad (114)$$

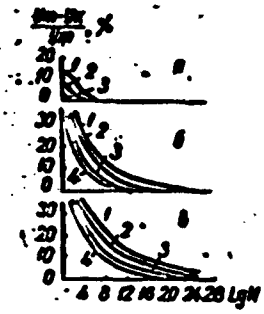

Fig. 25. Dependence of the relative error at different approximations to Formula (114) on the total number of defects N = NV: a - m = 3; b - m = 15; c - m = 25; 1 - for y ; 2 - for y_1; 3 - for y_2; 4 - for y_3.

If we neglect in the left side of Equation (114) all terms which contain σ^*/σ_u, which is correct in the case of a large number of defects in material N (for metals N is of the order of magnitude close to the number of grains, i.e., it approaches 10^{12} and more with regular dimensions of specimens), we will have

$$\frac{\sigma^* l}{m^m} = \overline{NV}\left(\frac{\sigma^*}{\sigma_u}\right)^{m+1} \qquad (115)$$

or

$$\sigma^* = \frac{A}{\sqrt[n]{V}}. \qquad (116)$$

where (52A)

$$A = \sigma_u\left(\frac{\sigma l}{m^m \overline{N}}\right)^{\frac{1}{m+1}};\quad n = m+1.$$

The formula thus obtained fully coincides with the Weibull Formula (96).

More accurate results can be obtained by taking into account the terms of the polynomial Φ^*, which contain σ_1^* in the first, second or higher degree. The error occurring depends on the number of defects in specimen $N = \bar{N}V$.

The greater this magnitude, the simpler the formula to be used in obtaining the required accuracy.

Shown in Fig. 25 are the results of calculating the error which is ontained in different approximations in the form of function $\frac{y_m - y_k}{y_m}$ of logN, where $y_m = \frac{\sigma^*}{\sigma_1^*}$, calculated without approximation according to Formula (114), and y_k is also a ratio, calculated according to an appropriately approximated formula: y_0 according to Formula (116), y_1 according to Formula (114) and so on.

The Theory of J. Fisher and J. Hollomon /66/

Whereas in the theories of Kontorova and Frenkel', as well as Weibull, in developing the basic equations only maximum normal elongation stresses are taken into account, in the theory of Fisher and Hollomon an attempts is made to take into account the effect of defects on strength in the case of a compound state of stress, considering the orientation of cracks. This theory, according to its assumptions, completely corresponds to the hypothesis of the "weak link."

As a condition of breakdown of a specimen the authors assume reaching in any crack, which is characterized by dimension c, of a critical stress, which they determine according to the Griffiths formula

$$\sigma_k' = Ac^{-\frac{1}{2}} .$$

In this work, the distribution of defects is written in the following form:

$$p\left(\frac{c}{h}\right) = e^{-\frac{c}{h}}. \qquad (117)$$

where h is constant.

Designating the relation $\sigma_k/Ah^{-\frac{1}{2}}$ by σ', we will find

$$\sigma' = \left(\frac{c}{h}\right)^{-1/2}. \tag{118}$$

Here σ' is the ratio of critical stresses for cracks of width c to those in a crack with width h.

From the function

$$p(\sigma) = p\left(\frac{c}{h}\right)\left|\frac{d\sigma}{d\left(\frac{c}{h}\right)}\right| \tag{119}$$

the curve of distribution of the corresponding critical stresses can be presented inthe form

$$p(\sigma) = \frac{2}{\sigma^3} e^{-1/\sigma^2}. \tag{120}$$

This equation shows that there is a most probable value of σ', and hence of σ_k when $\sigma' = (2/3)^{\frac{1}{2}}$ or when c/h = 3/2.

Assuming further that the element of the material experiences the action of the system of main stresses $\sigma_x = \sigma_y = \alpha\sigma_r > 0$, $\leqslant 1$, the authors find for the case of a single conventionally oriented crack in the specimen such an expression of the probability that the specimen does not break down:

$$\Pi = \int_0^{\infty} p(\sigma_r)\,d\sigma_r - \int_0^{1} p(\sigma_r)\left[1 - \sqrt{\frac{\sigma_r - \alpha}{1-\alpha}}\right] d\sigma_r \tag{121}$$

where

Function $p(\sigma_r) = p(\frac{\sigma_k}{\sigma_2})$ $\sigma_r = \sigma_k/\sigma_2$ can be presented in the form

$$p(\sigma_r) = \frac{2}{\beta^3\sigma_r^3} e^{-\frac{1}{\beta^2\sigma_r^2}}. \tag{122}$$

where

$$\beta = \frac{\sigma_r}{Ah^{-\frac{1}{2}}}.$$

Thus, the probability of breakdown of the specimen depends in this instance on parameters α and β and on the law of distribution of the dimensions of the crack, which was assumed in the form

$$p\left(\frac{c}{h}\right) = e^{-\frac{c}{h}}. \tag{54A}$$

If the specimen contains N cracks, the probability of its

breakdown under the effect of the system of stresses, cited above, will be in the form

$$P^{*}_{\alpha,0}(\beta)\,d\beta = N\Pi^{N-1}\left(\frac{\partial\Pi}{\partial\beta}\right)^{*}d\beta. \qquad (123)$$

In the work of Fisher and Hollomon, the probability of breakdown according to Formula (123) was determined for several values of N and three values of α.

The values of α were selected as follows: $\alpha = 0$ (simple elongation); $\alpha = 1$ (hydrostatic elongation); $\alpha = -1$ (elongation in the direction z and equal pressure in two other directions). For $\alpha = 0$, Equation (123) is reduced to the form

$$P^{*}_{\alpha,0}(\beta) = N\left[1-\int_{0}^{1}p(\sigma_1)\sqrt{\sigma_1}\,d\sigma_1\right]^{N-1}\left[\frac{\partial}{\partial\beta}\int_{0}^{1}p(\sigma_1)\sqrt{\sigma_1}\,d\sigma_1\right]; \qquad (124)$$

in case $\alpha = 1$

$$P^{*}_{\alpha,1}(\beta) = \frac{2N}{\beta^3}e^{-1/\beta}\left[1-e^{-1/\beta}\right]^{N-1}; \qquad (125)$$

in case $\alpha = -1$

$$P^{*}_{\alpha,-1}(\beta) = N\left[1-\int_{0}^{1}p(\sigma_1)\sqrt{\frac{\sigma_1+1}{2}}\,d\sigma_1\right]^{N-1}\times$$
$$\times\left[\frac{\partial}{\partial\beta}\int_{0}^{1}p(\sigma_1)\left(1-\sqrt{\frac{\sigma_1-1}{2}}\,d\sigma_1\right)\right]. \qquad (126)$$

The results obtained by the authors from the above formulas are given in Table 15. Cited in this Table are the values of the most probable relative strength β_p for $\alpha = 0;\ 1;\ -1$ in the interval $N = 10^0 \div 10^{20}$.

Table 15

N	β_p			$\frac{\beta_p(\alpha=1)}{\beta_p(\alpha=0)}$	$\frac{\beta_p(\alpha=-1)}{\beta_p(\alpha=0)}$
	$\alpha=0$	$\alpha=1$	$\alpha=-1$		
10^{20}	—	0,1473	—	—	—
10^{18}	—	—	—	—	—
10^{16}	0,1767	0,1647	0,1787	0,932	0,011
10^{14}	0,1905	0,1761	0,1928	0,924	1,012
10^{12}	0,2080	0,1902	0,2109	0,914	1,014
10^{10}	0,2312	0,2081	0,2352	0,900	1,017
10^{8}	0,2637	0,2325	0,2697	0,882	1,023
10^{6}	0,3140	0,2679	0,3243	0,853	1,033
10^{4}	0,4055	0,3265	—	0,805	—
10^{2}	0,6363	0,4490	—	0,706	—
10	1,00	0,5852	—	0,590	—
1	—	0,8165	—	—	—

Note: β_p is the most probable relative breakdown stress.

A shortcoming of this theory is its complexity which limits the possibilities of its utilization.

In other statistical theories, which make it possible to take into account the effect of the nonuniformity of the properties of the material on the integral characteristics of strength, as the criterion of breakdown conditions are assumed which differ from the conditions formulated above under the designation of the hypothesis of the "weak link." These theories include the statistics theory of strength of Volkov /69-72/, which makes it possible to explain certain laws observed in the breakdown of materials under conditions of compound state of stress, as well as the theory of Daniels /73/ on the strength of cables, and the theory of fatigue strength of metals of Afanas'yev /74/.

The Theory of S. D. Volkov /69-72/

In this theory the assumed criterion of breakdown is the infringement of the solidity of material unde the effect of elongation stresses in a certain relative part of the microvolumes of quasi-isotropic polycrystals.

Proceeding from energetic assumptions, the distribution of stresses in the microvolumes of polycrystals is given in this theory

in the form of the normal law

$$p(\sigma) = \frac{1}{\sqrt{2\pi}\Delta} e^{-\frac{(\sigma-\alpha)^2}{2\Delta^2}}, \qquad (127)$$

where α is the mean normal stress acting at the given cross-section; σ is the stress in microvolumes of the said cross-section; Δ is the mean quadratic deviation of the distribution of stresses in microvolumes.

The mean quadratic deviation is represented by the following function:

$$\Delta^2 = \theta = \theta_0 + kU, \qquad (128)$$

where k is constant (k = 1/6); U is the action of stresses of external forces in a unit of volume of the polycrystal; θ_0 is the module of distribution in the case of absence of external forces.

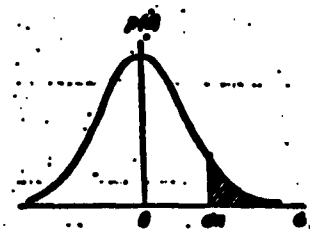

Fig. 26. Curve of distribution of stresses in microvolumes of polycrystal.

The relative number of microvolumes with stresses exceeding the resistance to breakdown (σ_n) in the planes of polycrystal, perpendicular to the action of stress α, will equal (Fig.26)

$$q = \frac{1}{2} - \frac{1}{\sqrt{2\pi}} \int_0^{\beta} e^{-\frac{z^2}{2}} dz \qquad (129)$$

and will be determined by the upper limit of integration

$$\beta = \frac{\sigma_n - \alpha}{\sqrt{\theta}}. \qquad (130)$$

The condition of breakdown of polycrystal is written in the following form

$$q = q_{kr} \qquad (131)$$

where q_k is the constant for the given material which does not depend on the nature of the state of stress.

Thus, upon pressing the specimen along one of the axes ($\sigma_1 = 0$, $\sigma_2 = 0$, $\sigma_3 < 0$), the relative number of broken down microvolumes along planes perpendicular to axis 1, will equal

$$q_1 = \frac{1}{2} - \frac{1}{\sqrt{2\pi}} \int_0^{y_1} e^{-\frac{x^2}{2}} dx; \tag{132}$$

$$y_1 = \frac{\sigma_3}{\sqrt{\theta}}. \tag{133}$$

where, in accord with Eq.(128)

$$\theta = t_0 + \frac{k}{2E}\sigma_3^2 \tag{134}$$

Then

$$y_1 = \frac{\sigma_3}{\sqrt{t_0 + \frac{k}{2E}\sigma_3^2}}. \tag{135}$$

The relative number of broken down microvolumes in the plane perpendicular to axis 3,

$$q_3 = \frac{1}{2} - \frac{1}{\sqrt{2\pi}} \int_0^{y_3} e^{-\frac{x^2}{2}} dx, \tag{136}$$

where

$$y_3 = \frac{\sigma_3 - \sigma_0}{\sqrt{t_0 + \frac{k}{2E}\sigma_3^2}}. \tag{137}$$

Comparing y_1 with y_3 taking into account $\sigma_3 < 0$, we can come to the conclusion that $q_1 > q_3$ and breakdown will take place in a plane parallel to the axis of the specimen.

Breakdown of this form is often observed in testing for pressing brittle metalloceramic materials (see Fig. 20,a).

This form of breakdown can be explained by the fact that as a result of anisotropy of mechanical properties of the crystal in imposing external loads, in a part of such crustals, in planes perpendicular to axis 1, there appear stresses both of pressing as well as elongation, although mean stress will equal zero.

Acting on the basis of these assumptions, one can very convincingly explain certain laws governing the breakdown of metals under other forms of state of stress.

This theory does not take into account the effect of micro-cracks with different concentration of stresses on strength. It assumes as the criterion of breakdown the breach of continuity in a certain relative part of microvolume regardless of its location, while in breakdown of materials the essential role is played by the probability of finding a certain number of such breakdowns in a series and such crack reaching critical dimensions.

The Theory of Daniels /73/

In work /73/ Daniels investigated the problem of strength of cable consisting of n parallel filaments of equal length, thus attached with their ends, that all filaments experience equal stretch during elongation.

Strength of cable is understood to mean the maximum load S which it can withstand without breakdown. The cable does not break down if there is a whole number of filaments (r) with a strength exceeding S/r. The filaments of which the cable is made up as assumed to be a fortuitously selected batch out of an infinite number of filaments with the known law of distribution of their strength.

The probability that a filament will not break down under load s(s = S/n) is written in the form

$$\delta(s) = 1 - [1 - \beta(s)]^N, \qquad (138)$$

where N is the number of independent, successively joined elements in the filament; $\beta(s)$ is the law of distribution of strength of these elements.

Daniels assumed that all filaments of which the cable consists,

have identical curves in the coordinates of load and elongation, that the probability of a filament breaking down under load is such that /1 - b(s)/ proceeds toward zero faster than 1/s, etc. He also found that the strength of union (S) has a distribution which approximates for large n the normal law with mean values

$$S_s = ns_s[1 - b(s_s)] \tag{139}$$

and mean quadratic deviation

$$\Delta = s_s\sqrt{nb(s_s)[1 - b(s_s)]} \tag{140}$$

where s corresponds to the maximum value of s/1 - b(s)/.

The Theory of M. M. Afanas'yev /74/

This theory provides the solution of the problem of the appearance of a fatigue crack in polycrystal taking into account the nonuniformity of strength properties and stress of microvolumes of the material.

This theory assumes that a fatigues crack appears as a result of joining into one whole of a series of microscopic breakdowns in individual grains *).

Afanas'yev believes that the cause of breakdown lies in a strengthening produced by cyclical load which causes a breakdown at the instant of normal stresses reaching of resistance of the material to break-off.

This theory assumes as the criterion of breakdown the breach of unity in n grains which lie alongside of each other. If volume V

*) In this case grain designates a microvolume of material which possesses identical properties in all points.

contains Z grains, the number of units with n grains will equal Z : n.

The number of grains with stress exceeding resistance to break-off equals

$$m = \int_{\sigma_{br\text{-}off}}^{\infty} p\left(\frac{\sigma}{d}\right) d\left(\frac{\sigma}{d}\right). \tag{141}$$

where $\frac{\sigma}{d}$ is the relative stress; $p\left(\frac{\sigma}{d}\right)$ is the curve of distribution of relative stresses in the grains. The number of units with n grains which have a stress exceeding $\sigma_{br\text{-}off}$ will equal $\frac{m}{n}$.

Then the probability of finding n grains with m in a row is determined as the ratio of the number of combinations with m in n to the number of combinations with Z in n

$$W = \frac{C_m^n}{C_Z^n} = \frac{m!(Z-n)!}{Z!(m-n)!} \approx \left(\frac{m}{Z}\right)^n. \tag{142}$$

If we take into account that the parameters of the equation of the curve of distribution of stress in the grains are selected in such a manner that the plane of the curve, and hence the magnitude of Z equal unity, we can write

$$W = \left[\int_{\sigma_{br\text{-}off}}^{\infty} p\left(\frac{\sigma}{d}\right) d\left(\frac{\sigma}{d}\right)\right]^n. \tag{143}$$

The condition of breakdown is written in the form

$$W\frac{Z}{n} \geq 1 \tag{144}$$

or

$$CWV \geq 1, \tag{145}$$

where V is the volume of the specimen and C is the coefficient of proportionality.

Proceeding from these considerations, Afanas'yev explained certain laws which are observed in fatigue breakdown of metals (effect of dimensions of specimens, form of state of stress, clean surfaces, concentration of stresses, etc.).

The methods of mathematical statistics are now widely used in investigating the problem of fatigue, as well as in other aspects, primarily for deep analysis of the results of fatigue tests and devising appropriate methods of their processing /50, 51, 75-81/.

These methods are used in investigating the laws governing the dispersion of energy in material under vibration /82, 83/, the study of nonuniformity of the flow of plastic deformation in microvolumes of material /84-86/, in the study of strength of material taking into account the time of load application /87/ etc.

Chapter Four

Investigation of the Laws Governing the Breakdown of Heat Resistant Metalloceramic Materials

In this chapter we cite the results of investigations made by the Institute of Metaloceramics and Special Alloys Acad Scien UkSSR, for the purpose of studying the laws governing the breakdown of heat resistant metalloceramic materials, taking into account their structural heterogeneity.

In order to take into account the effect of microdefects on strength, use was made of the statistical theory of strength of Weibull, the physical prerequisites of which largely correspond to the properties of heat resistant metaloceramic materials, and the mathematical apparatus is very simple.

Considerable attention was paid to the method of testing brittle materials for strength, since the existing methods of testing brittle materials are mostly unsuitable for testing metalloceramic materials for strength at high temperatures.

1. Composition and Technology of Production of Materials subjected to Tests

Three types of materials were tested for strength, whose heat resistant components were: chromium carbide Cr_3C_2, Silicon carbide SiC, and Titanium carbide TiC.

Chromium, silicon and titanium carbide, as evident from Table 2, have a high melting temperature, high heat resistance, and other advantageous properties. These carbides are considered in literature as a possible base for the production of new turbo-blade materials, capable of operating in temperatures of 1000°C and higher. Utilization of chromium, titanium and silicon carbide as turbo-blade material is made difficult by their lack of plasticity, therefore heat resistant materials containing the above as base, include, as we have noted, other components, the basic purpose of which is to give the material the required plasticity.

The investigated metal-ceramic alloy on the base of chromium carbide /88, 90/ is a typical cermet consisting of chromium carbide and a metal binder - nickel.

By changing the percentage content of these components, one can obtain material with widely different properties.

As a rule, the increase of the content of the metal binder produces an increase of plasticity, and hence impact strength, although the strength of these material at high temperatures drops to a certain degree.

As investigations have shown, which were conducted at the Institute of Metal-ceramics and Special Alloys Acad Scien UkSSR, a promising material on the base of Cr_3C_2 for use in high temperatures is a metal-ceramic alloy containing 85% Cr_3C_2 and 15% Ni. It possesses fairly high characteristics of strength at temperatures above 1000°C and is also capable of withstanding a considerable number (over 200) of sharp temperature changes according to the following regime: heating to a

temperature of 1050° (15 sec), cooling in a strong stream of carbonic acid gas to a temperature of 400-500° (20-25 sec) /90/.

This material breaks down to a temperature of 1000° without any visible traces of remaining deformation. In this connection, in order to investigate the laws governing the breakdown of brittle metalloceramic materials, the composition of this content was selected.

The specimens for investigations were made, as usual, in powder metallurgy, by pressing batches consisting of powders of chromium carbide and nickel in special press molds with subsequent baking of the prepared material.

Chromium carbide was used obtained by direct regeneration of chromium oxide with lampblack. Its chemical composition is as follows: 85.5-86.8% Cr, 13.0-13.6% C, not over 0.3% C (free). Granularity - below 40 microns; purity of nickel powder not below 98% and granularity below 40 microns.

The powders of chromium carbide and nickel were subjected to moist grinding and mixing over a period of 50 hrs in alcohol (350 ml alcohol for 1 kg mixture).

Then the batch was dried and mixed with a solution of rubber in gasoline (for 1 kg of batch 200 ml 5% solution of rubber). The mixture obtained was dried and passed through a sieve with aparture dimensions of 417 microns. The batch thus prepared is satisfactorily friable and evely fills the press-mold.

Pressing of the specimens was conducted under pressure of 1.25 t/cm^2. The batch for pressing was calculated according to the formula

$$G = \gamma V k, \qquad (146)$$

where is the specific gravity of the alloy; k is the coeff cient accounting for losses in pressing, burning of rubber in baking and

allowance for processing. If there is no allowance for processing, k = 1.01 -- 1.03; V is the volume of the finished product.

The specific gravity of the alloy γ can be approximately calculated according to the formula

$$\gamma = \gamma_{Cr_3C_2} \frac{\Pi_{Cr_3C_2}}{100} + \gamma_{Ni} \frac{\Pi_{Ni}}{100} \qquad (147)$$

where $\gamma_{Cr_3C_2}$ is the specific gravity of chromium carbide (6.68 g/cm^3); γ_{Ni} is the specific gravity of nickel (8.9 g/cm^3); Π is the percentage of carbide and nickel in the alloy.

Baking of the preparations was done in Tamman ovens in an atmosphere is dried hydrogen.

Baking temperature was close to 1300°, time 50-80 min. The temperature and time were selected for each lot of specimens in such a way, as to attain a maximum solidity of the alloy.

The microstructure of the material thus obtained is shown in Fig. 27, magnified 500 times.

Fig. 27. Microstructure of metaloceramic material on a base of chromium carbide (X500): a - 85% Cr_3C_2; 15% Ni; b - 60% Cr_3C_2; Ni - 40%.

As can be seen from Fig. 27 a, the alloy consists of an almost solid griddle of carbide grains with individuals splashes of nickel. In Fig. 27 b, we show for comparison the microstructure of a similar alloy

with a large content of binder (40% Ni). In preparing specimens, special attention was paid to the control of the quality of finished products.

For each lot of specimens, a chemical analysis of material was made, the solidity of baked specimens was determined, and the microstruture and porosity of the material was checked. The permissible deviation of solidity of material, determined by hydrostatic weighing, was not greater than the calculated by 1.5 to 2%.

The metal-ceramic alloy containing 85% Cr_3C_2 and 15% Ni has the following properties /89/:

Elasticity module, kg/mm^2	$3 - 3.3 \cdot 10^4$
Hardness R_A	86 - 90
Impact elasticity, kgm/cm^2	0.1 - 0.2
Specific gravity, g/cm^3	7.0
Heat conductivity, cal/cmsec degree	0.03
Coefficient of linear expansion	$12 \cdot 10^{-6}$
Electrical resistance, ohm $\cdot$ mm^2/m	0.63
Magnetic properties	nonmagnetic

The material on the base of silicon carbide was also produced by the powder metallurgy method, i.e., a batch was prepared from which preparations of specimens were pressed, and subsequently subjected to thermal processing.

In this case the batch was from graphite processed with bakelite. Specimens were pressed in molds at insignificant specific pressures. After drying they were subjected to a soaking in melted silicon in Tamman ovens in an atmosphere of dried hydrogen at a temperature of 2000°.

Table 16

Composition	Content %			E, kg/mm^2	g/cm^3
	SiC	C_{free}	Si_{free}		
1	65.83	25.13	9.04	$1.9 \cdot 10^4$	2.8
5	54.39	33.37	12.24	$1.1 \cdot 10^4$	2.4

As a result of soaking a material was obtained having three phase components: silicon carbide (SiC), free silicon (Si) and free graphite (C).

Chaging the sieve composition of the batch, porosity of the preparation, method of soaking, etc., one can obtain material of different strength and stability against heat impact. The characteristic of materials of this composition is that the more free graphite they contain, they lower their mechanical strength and the higher their stability against heat impact.

Fig. 28. Microstructure of ceramic material on a base of silicon carbide (X200): a - composition 1, b- composition 5.

Six different compositions were made for the tests, with identical phase components, but in different ratios.

If we accept as the basis of classification of these compositions the sieve composition of the batch which was used for pressing prepara-

tions, composition 1 was made from fractions - 104 microns and + 50 microns; composition 2 from fractions -50 microns; composition 3 from fractions -208 and +50 microns, composition 4 from fraction -208 microns and +147 microns, and composition 5 from fractions-833 microns and +208 microns.

The chemical composition and some properties of two of these compositions are given in Table 16.

Micro-polished surfaces of compositions 1 and 5 are shown in Fig. 28 enlarged 200 times.

These pictures clearly show three phase components: dark areas - graphite, grey - silicon carbide, and white - silicon.

In this instance particular attention was paid to obtain identical material in specimens of different shape and dimension.

This was achieved by selecting appropriate regimes of soaking, as well as by control of the quality of specimen production.

Control was maintained over the chemical composition, shrinkage after soaking, solidity and microstructure of the material. To a limited extent we also investigated the strength of cermet on a base of titanium carbide; this material contained 70% TiC and 30% metal binder /90/.

The method of making specimens from this material was analogous to the above described method of making specimens from metaloceramic material on the base of Cr_3C_2.

2. Method of Investigating the Strength of Brittle Material under Conditions of Room Temperature and High Temperatures

The most widespread form of test for strength is: elongation, bend, twisting and pressing. The latter, pressing, due to great difficulties of realizing it in pure form, as well as due to the impossibility

corparing the obtained results with the characteristics of the strength of material found in other forms of tests, can be only considered as of secondary importance.

More reliable results can be obtained in tests for elongation, bend and twisting.

Simultaneously, however, the strength characteristics of brittle metalloceramic materials, found under these forms of load, are correct only in these instances, if during their determination sources of error were eliminated, which could have distorted the true results.

The possible sources of error are: changes of properties of the material in the process of making specimens from one lot and from several lots, inaccurate designation of actual stresses and state of stress at the instant of specimen breakdown, comparing obtained results without taking their dimensions into account, diagrams of loading, rate of load application, medium, etc.

The method of producing heat resistant metalloceramic materials, in which every specimen (or part) is individually made, massing successively through the stage of pressing and baking, requires particularly care in these operations, otherwise the properties of the material of different specimens from a single lot and from many lots, with an identical chemical composition and nominally identical production technology - will be different.

Differences of properties of material can be caused by different degree of purity of the initial raw material, pressing pressure, porosity, method of baking, etc. All these questions are considered in detail in special literature on powder metallurgy /8,9, 28/.

The main objective of the investigations on the laws governing breakdown of heat resistant metalloceramic materials is reduced in this part to a desire to adhere to a maximum similarity of technology of

specimen production, and reliable control of the material obtained in specimens and parts.

Inaccurate designation of actual stresses and state of stress during tests can be caused by the following factors:

a) Improper shape of specimens accepted for the determination of mechanical properties of the material, which can cause a considerable macro- and micro-concentration of stresses in transit areas, as well as in the places of contact of specimens with parts of pressing tools;

b) Deviation of shape and dimensions of specimens from the nominal, which can take place in the process of making metaloceramic specimens;

c) Using insufficiently accurate formulas to determine stresses at the instant of breakdown, which occurs, for example, in calculating the stresses of bending according to the usual formulas of resistance of material in the case of material with different modules of elasticity during elongation and pressing;

d) Improper construction of implements to be used in testing brittle metaloceramic metarials for strength.

Below we consider the effect of these factors on the strength characteristics under different forms of load, and we describe the method of tests used in this work.

Elongation. The selection of the shape and dimensions of specimens to determine the strength on elongation of brittle metaloceramic materials under conditions of room and high temperature is a fairly difficult undertaking.

In addition to the general requirements of specimens for testing brittle material, it is imperative to take into account the specifics of producing the specimens by the powder metallurgy method, the extreme hardness of heat resistant metaloceramic materials, and hence also the difficulties of mechanical processing of specimens, the need of heating

them in tests to temperatures of the order of 1500° and higher, etc.

In literature /29, 53, 91-94/, with reference to tests of brittle materials for elongation, the most frequently considered types of specimens are those give in Fig. 29.

These specimens have the following shortcomings and advantages. Specimen of type I, according to the opinion of a majority of researchers, is unsuitable for elongation tests of brittle materials.

In this shape of specimen, near the aperture through which the load is transmitted to the specimen, there is a great concentration of stresses, and specimens break down outside of the operating part.

To remove this, it is necessary to greatly increase the size of the head of the specimen, which creates difficulties in making them by the powder metallurgy method.

The concentration of stresses near the apertures in specimens of this type was investigated in detail by Frokht /95/ by the method of photo-elasticity, predicated on the following factors:

a) Ratio of the diameter of the aperture to the width of the plate 2r/D;

b) Size of clearance between the cylinder and aperture in the plate;

c) Ratio of distance between the upper block surface of the plate and the center of the aperture to the width of the plate H/D.

The coefficient of stress concentration was calculated by means of the formula

$$K = \frac{\sigma_{max}}{\sigma} = \frac{\sigma_{max}(D-2r)t}{P}, \qquad (148)$$

where σ_{max} are the maximum stresses of elongation on the contour of the aperture; P is the load on the specimen; D, r, H, t are geometric dimensions (see Fig. 30).

The results obtained by Frokht are given in Fig. 30.

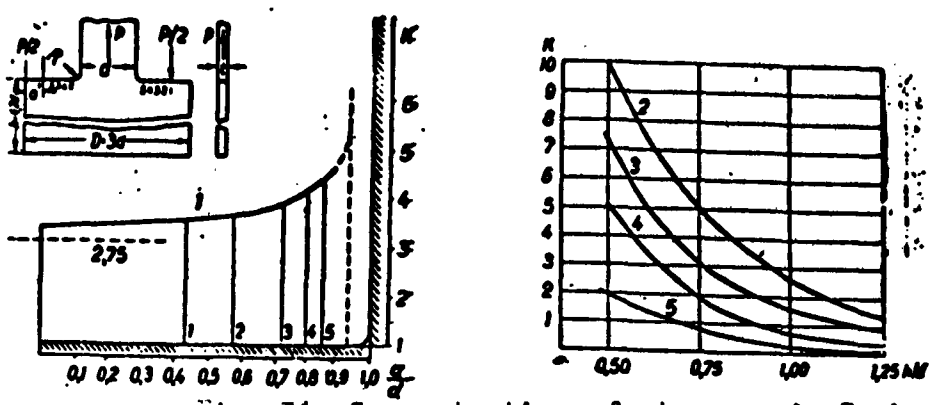

Fig. 31. Concentration of stresses in T-shaped head:

1 - depending on distance of the point of applying load to place of transition; 2-5 - depending on ratios h/d;

2 - $\frac{D}{d} = 3.0$; 3 - $\frac{D}{d} = 2.5$; 4 - $\frac{D}{d} = 2.0$; 5 - $\frac{D}{d} = 1.5 (\frac{R}{d} = 0.075)$

These data show that the concentration of stress near the aperture is very great and its reduction is associated with a significant increase of the dimensions of the head of the specimen.

The shortcoming of specimen type II (see Fig. 29) also lies in the considerable concentration of stresses in the places of transition from the operational part of the specimen to the head, which requires considerable increase of the radii of rounding R_1 and R_2 /53, 92/.

The coefficients of concentration of stresses in this case, are given in Fig 31, after the data of Hetenyi /96/. Here $\frac{R}{d} = 0.075$, $\sigma_{max} = k \sigma_{nom}$, and $\sigma_{nom} = \frac{P}{td}$.

Curve 1 (Fig.31) shows the dependence of the coefficient of concnetration of stresses on the distance of the point of application of the load to the place of transition, and curves 2-5 - the dependence of this magnitude on the ratios D/d and h/d in the case of equally distributed load.

Specimen of type III)see Fig. 29 /93, 94/ is very difficult to produce by the powder metallurgy method with sufficient accuracy without subsequent labor-consuming reduction of its surfaces.

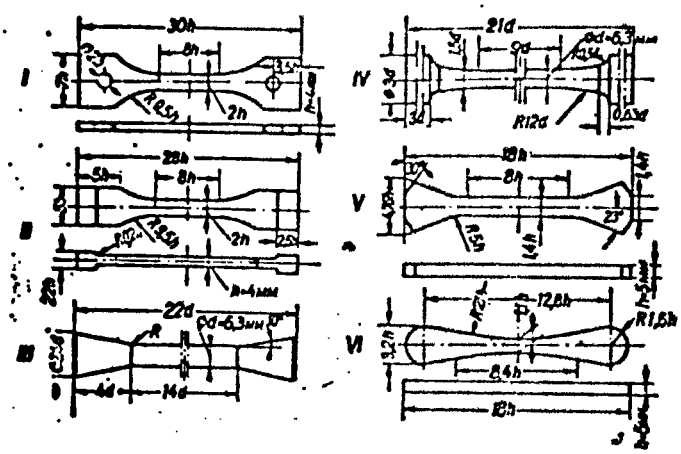

Fig. 29. Various types of specimens used in testing brittle materials for elongation.

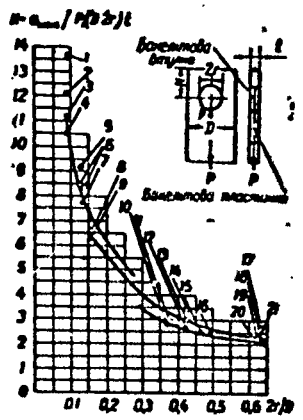

Fig. 30. Coefficient of concentration of stresses K for an elongated plate with an aperture through which the load is transferred: 1, 2, 3, 5, 6, 8, 11, 17, 19 - results obtained when there was clearance between the cylinder and plate; 4, 7, 9, 10, 12, 13, 15, 18, 20, 21 - results obtained in absence of clearance and tension;

$1-4-\frac{H}{D}=0.36$; $5-7-\frac{H}{D}=0.29$;
$8,9-\frac{H}{D}=0.39$; $10-12-\frac{H}{D}=1.05$;
$13,14-\frac{H}{D}=0.57$; $15-\frac{H}{D}=1.14$;
$16-\frac{H}{D}=1.29$; $17-18-\frac{H}{D}=0.86$,
$19-21-\frac{H}{D}=1.33$.

A shortcoming of this type of specimen is the considerable concentration of stresses at the surface of contact /92/.

Special attention must be paid to a tight adhesion of the surfaces of heads of speciemens to the vises, otherwise, as can be seen from Fig. 32, there is a possible very high concentration of stresses at individual overstressed points. The effect of this factor must be taken into account also in using specimens of other types.

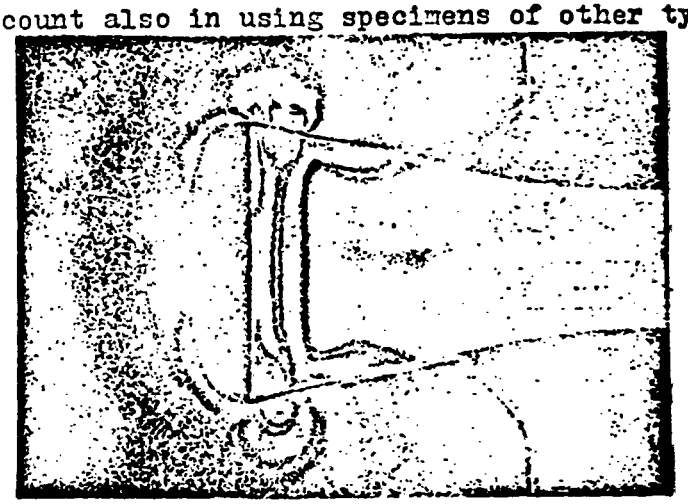

Fig. 32. Concentration of stresses in the head of a "swallow-tail" type of specimen.

Satisfactory results were obtained in using specimens type IV in tests for elongation /53/.

Nevertheless, the complexity of making similar specimens from hard-to-process materials by mechanical means makes the advisability of their use doubtful.

The Institute of Metalloceramics and Special Alloys Acad Scien UkSSR successfully uses specimens V and VI for elongation tests under room and high temperature conditions. Their shape and dimensions are given in Fig. 29.

The advantages of these specimens lie in the simplicity of making them by the powder metallurgy method, absence of sharp transfers which excludes concentration of stresses in the operational part of the specimen, uncomplicated processing of surfaces by ultrasound and electro-

spark method, which are the most promising in this case.

The shortcoming of these specimens is the considerable concentration of stresses occurring in the heads, which requires reduction of the contact surfaces.

The shape of specimen type VI is particularly convenient in using the method of heating specimens by direct electric current, where the zones of maximum temperatures and stresses coincide, and there is a reduced probability of breakdown in cross-sections close to the heads, in which the greatest temperature drop occurs.

Among other methods of heating specimens to reach temperatures of 1500° and higher, worthy of note are: heating by means of external heaters which can be tungsten, molybdenum, tantalum, graphite, etc. However, tests become very complicated in connection with the need to provide a sheltered atmosphere for high melting metals and graphite which easily oxidize at high temperatures; in addition, reaching extremely high temperatures, required for the testing of some alloys given in Table 2, as altogether impossible if we use high-melting metals as heaters.

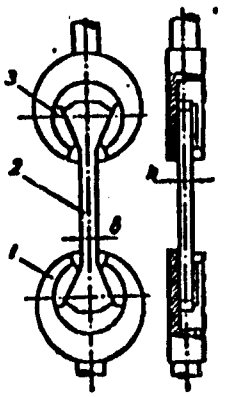

Fig. 33. Diagram of attaching specimens in vises in tests for elongation: 1 - heads of vises; 2 - specimen; 3-thrust bearings.

A diagram of attaching specimens of type V and VI in vises, which is used by the Institute of Metaloceramics and Special Alloys Acad Scien UkSSR in testing such specimens, is shown in Fig. 33.

Specimen 2 is attached in the heads of vises 1 by means of cylindrical thrust bearings 3, the dimensions of which are so selected, that when the specimen is mounted they take part in the pressing with the entire surface of the cylindrical heads of the vises.

Changing the dimensions of these thrust bearings, we can calculate the equal change of dimensions which takes place in their thermal processing.

In using these vises, attention should be paid in particular to the contact between the specimen and thrust bearings, otherwise considerable bending stresses may be superimposed on the elongation stresses.

The use of specimen IV and VI)see Fig.29) requires, as in other instances, careful control of their shape and dimensions after they are made, in order to avoid essential errors in determining the limit of endurance.

Thus, if specimen V has a bent longitudinal axis with an error of bend y, additional stresses of bend appear in tests, which can be determined by the formula

$$\sigma_{bend} = \frac{6Py}{bh^2}. \qquad (149)$$

The allowable error in neglecting this factor, will equal

$$\Delta\sigma = \frac{\sigma_{all} - \sigma}{\sigma_{all}} 100\% = 6\frac{y}{b} \cdot 100\%. \qquad (150)$$

where σ_{allow} are the total stresses of bend and elongation which occur in the center part of the specimen; σ - elongation stresses.

Let y = 0.2 mm and b = 7 mm; then

$$\Delta\sigma = 17.1\%.$$

If the actual thickness of the specimen does not correspond to the calculated thickness (Fig.33), we will have eccentric elongation. Here

$$\sigma_{bend} = \frac{P\Delta h6}{2bh^2}, \tag{151}$$

and the rror will be determined by the following function:

$$\Delta\sigma'' = \frac{\Delta h3}{h} 100\%, \tag{152}$$

where Δh is the difference in height of the nominal and actual specimens. If h = 5.5 mm and Δh = 1 mm, then $\Delta\sigma''' = 60\%$. The magnitudes of error cited here will occur during breakdown, as a rule only if the specimen does not deform. With considerable lengths the effect of this factor through deformation was weaker.

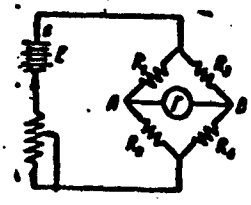

Fig. 34. Electric diagram of measuring deformations by means of pickoffs of ohmic resistance.

The effect of the accuracy of specimen preparation on the magnitude of stresses was investigated on specimens of type V (see Fig. 29) of metalloceramic alloy, consisting of 85% Cr_3C_2 and 15% Ni.

Investigations were conducted by means of tenso-pickoffs of ohmic resistance, cross-bar for measuring deformation "Orion" EMG 2353 type and taring beam whose one-millimeter buckling corresponds to

the relative deformation $\varepsilon = 6.0 \cdot 10^{-4}$. The buckling of the beam was measured with an accuracy of 0.01 mm. The principal diagram of measuring deformation by this method is shown in Fig. 34 /97, 98/.

If we observe condition

$$R_1R_4 = R_2R_3 \qquad (153)$$

then the bridge is balanced, i.e., there is no difference of potentials between points A and B.

If however, one of the resistors, for example, R_1 represents a pick-off of ohmic resistance glued to the specimen, then under a load of the specimen the resistance of the pick-off will change to magnitude ΔR_1 and the galvanometer will indicate a surrent in arm AB.

The unbalance of the bridge can be removed if we utilize as resistance R_3 an identical pick-off glued to the taring beam, which makes it possible to deform the pick-off by a known magnitude. This pick-off is also a temperature compensator.

Applying a load to the specimen and achieving a balance of the bridge by means of the taring beam, we can determine the deformation of the specimen at the place of the attachment of the pick-off.

The accuracy of measurement of the deformation will depend on the properties of the ohmic resistance pick-off, sensitivity of the deformation measuring bridge and sensitivity of the taring attachment.

In this case one mark on the galvanometer corresponded to the relative deformation $\varepsilon = 6 \cdot 10^{-6}$ (the sensitivity of the taring beam was indicated above).

In measuring elongation deformation, two pick-offs, consecutively joined, were glued onto the specimen which was elongated, from two opposite ends and were plugged into the bridge system as resistance R_1, two other pick-offs, also consecutively joined, were glued onto the elongated filaments of the taring beam and plugged into the dia-

gram as resistance R_3.

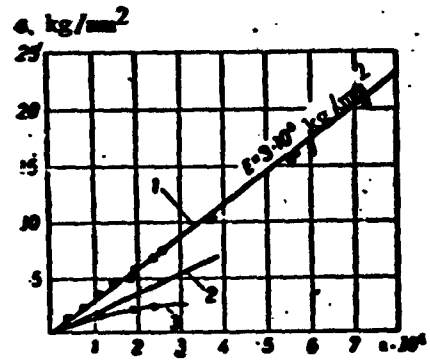

Fig. 35. Effect of inaccuracy of production of specimens on stress 1 - function of stress and deformation (circle - elongation; triangle - pure bend, elongated filaments; cross - pure bend, compressed filaments); 2 - function according to Formula (152); 3 - Experimentally determined function.

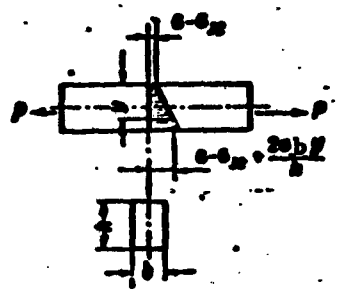

Fig. 36. Eccentric elongation of rectangular specimen with cross-section.

With this diagram of measurement we exclude the deformation of bend and measure only the deformation of elongation.

On the basis of results obtained, we determined the module of elasticity of the material (straight line, Fig. 35).

Bend deformation was measured by using two pick-offs of ohmic resistance, glued onto the specimen from two opposite sides; one of the pick-offs was plugged into the system as resistance R_1, and the other as R_3.

In this case deformation was directly shown by indications of the galvanometer of the deformation measuring bridge. The results obtained in these investigations are shown in Fig. 35. Straight line 2 corresponds to function (152) set up in coordinates σ' (stress of bend) - ε (deformation of pure elongation) for h = 5 mm and Δh = 1 mm; curve 3 is set up in the same coordinates according to experimental data.

The change of thickness of the specimen h was imitated by removing appropriate washers which were placed between the specimen of the area of the heads of vises (see Fig. 33). The data obtained indicate that the error experimentally observed is much smaller than it would appear from Formula (152). Also plotted on Fig. 35 are the results of determining the function of stresses and relative deformation on the surface of the specimen in the case of loading according to the diagram of pure bend. Deformation was measured both on compressed, as well as elongated filaments.

In eccentric application of loads to specimens, made of very heterogenous material, the strength of the specimens can be found in the following manner.

Using the formulas of the statistical theory of strength of Weibull, we can write for the case of pure elongation (96)

$$\sigma^0 = \frac{\sigma_0 l_0}{\sqrt[m]{lm}}. \qquad (72A)$$

In the case of eccentric application of load to specimen type V (Fig. 29) for $\alpha = \frac{\sigma_{bend}}{\sigma} < 1$ we will have (Fig. 36)

$$B = \int_V \left(\frac{\sigma}{\sigma_0}\right)^m dV. \tag{72B}$$

where

$$dV = lbdy; \quad \sigma = \sigma - \sigma_{allow.\ bend.} + \frac{2\alpha_{bend}\, y}{h}. \tag{72C}$$

Then the expression for the "chance of breakdown" will be written in the form

$$B = lb\left(\frac{1}{\sigma_0}\right)^m \int_0^h \left(\sigma - \sigma_{bend} + \frac{2\alpha_{bend}\, y}{h}\right)^m dy. \tag{72D}$$

Following integration

$$B = \frac{V}{2\alpha(m+1)}\left[(1+\alpha)^{m+1} - (1-\alpha)^{m+1}\right]\left(\frac{\sigma}{\sigma_0}\right)^m. \tag{154}$$

therefore, the most probable value of brittle strength, calculated according to Formula (91), with eccentric application of load will be

$$\sigma_1^\circ = \frac{\sigma_0 l_m}{V^{1/m}}\left[\frac{2\alpha(m+1)}{(1+\alpha)^{m+1} - (1-\alpha)^{m+1}}\right]; \tag{155}$$

$$A = \frac{\sigma^\circ}{\sigma_1^\circ} = \frac{\left[(1+\alpha)^{m+1} - (1-\alpha)^{m+1}\right]^{1/m}}{[2\alpha(m+1)]^{1/m}}. \tag{156}$$

Shown in Fig. 37 are the values of magnitude A depending on the coefficient of uniformity m for different values of . This ratio is close to 1 + α only at m $\to \infty$.

In the case of eccentric application of load to specimen type V (Fig. 29) for $\varkappa = \frac{\sigma_{bend}}{\sigma} < 1$ we will have (Fig. 36)

$$B = \int \left(\frac{\sigma}{\sigma_0}\right)^m dV. \tag{72B}$$

where

$$dV = lbdy;\ \sigma = \sigma - \sigma_{allow.\ bend} + \frac{2\sigma_{bend}^{\ }y}{h}. \tag{72C}$$

Then the expression for the "chance of breakdown" will be written in the form

$$B = lb\left(\frac{1}{\sigma_0}\right)^m \int_0^h \left(\sigma - \sigma_{bend} + \frac{2\sigma_{bend}^{\ }y}{h}\right)^m dy. \tag{72D}$$

Following integration

$$B = \frac{V}{2a(m+1)}\left[(1+a)^{m+1} - (1-a)^{m+1}\right]\left(\frac{\sigma}{\sigma_0}\right)^m. \tag{154}$$

therefore, the most probable value of brittle strength, calculated according to Formula (91), with eccentric application of load will be

$$\sigma_i^{\circ} = \frac{\sigma_0 l_m}{V^{1/m}}\left[\frac{2a(m+1)}{(1+a)^{m+1} - (1-a)^{m+1}}\right]; \tag{155}$$

$$A = \frac{\sigma^{\circ}}{\sigma_i^{\circ}} = \frac{\left[(1+a)^{m+1} - (1-a)^{m+1}\right]^{1/m}}{\left[2a(m+1)\right]^{1/m}}. \tag{156}$$

Shown in Fig. 37 are the values of magnitude A depending on the coefficient of uniformity m for different values of . This ratio is close to 1 + α only at $m \to \infty$.

Taking into account errors determined according to Formula (250) is quite difficult, since it is not easy to determine the arrow of buckling, therefore specimens with these deformations should be removed from tests.

The error determined according to Formula (152) can be easily removed by processing the specimens or selection of appropriate washers.

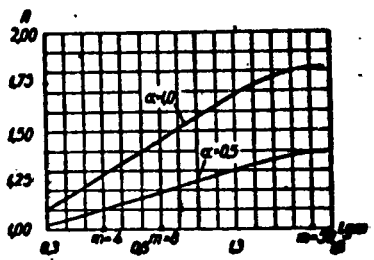

Fig. 37. Sensitivity to eccentricity of load application as a function of coefficient m.

If these operations are carried out, experiments have shown that stresses of bend will be insignificant (2-3%) and cannot distort of the results of elongation tests.

Tests of metaloceramic materials for elongation, as well as experimental investigations of the effect of inaccuracy of specimens on strength characteristics were conducted by means of a device shown on Fig. 38, which makes it possible to make tests in room, as well as high temperature. Specimen 9 is attached in vises cooled by water, by means of thrust bearings. The latter are lubricated with a graphite paste, which makes it possible for the specimen to self-align. In addition to this joint, there are spherical joints in places of juncture of traction rods with the press vises.

Current and cooling water is supplied through flexible attachments.

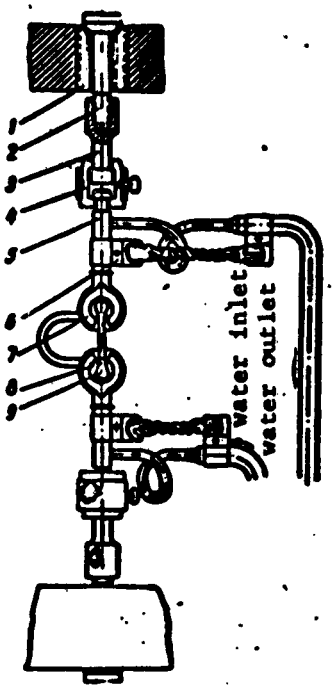

Fig. 38. Apparatus for elongation tests of specimens at room and high temperature: 1 - insulator; 2, 3, 5 - traction rods; 4 - joint; 6 - water-supply hose; 7 - head of vise; 8 - thrust bearing; 9 - specimen.

The electric diagram of heating specimens by passing electric current directly through them, which was used in elongation tests, as well as twisting and bend, is shown in Fig. 39.

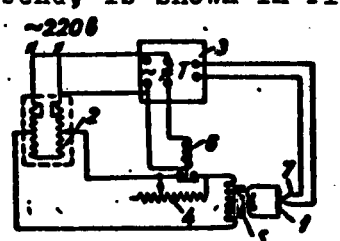

Fig. 39. Electric diagram of heating specimens by direct passage of electric current

1 - specimen; 2 - tension variator; 3 - control millivoltmeter; 4 - rheostat; 5 - heater transformer; 6 - magnetic starter; 7 - thermocouple or radiation pyrometer.

Elements of automatic maintenance of constant temperature were used whenever it was necessary to sustain temperature over long periods. Thermocouple or radiation pyrometer indicators were used only for temperature control.

Temperature was measured by means of type OPPIR-09 optical pyrometer, entering appropriate corrections for blackness of radiation of the specimen material. Tests were carried out on hydraulic press type "BLW" with scale markers of strength measurement in 2.5 kg.

Specimens type VI (see Fig. 29) were used. Stresses in the specimen at the instant of breakdown for calculated for mean cross-section, regardless of the location of the breakdown within the range of its operational part, which makes it possible to use the previously derived Formula (103) in the analysis of laws governing breakdown.

Bend. Tests for bend are usually carried out by either of the two methods shown in Figs. 22 and 23.

Resistance of materials gives widely known formulas for the determination of normal and tangent stresses in a beam of rectangular cross-section.

Pure bend

$$\sigma_{bend} = \frac{M_z y}{I_z}; \quad \tau = 0. \tag{157}$$

bend by concentrated force

$$\sigma_{bend} = \frac{M_z y}{I_z}; \quad \tau = \frac{Q}{2I_z}\left(\frac{h^2}{4} - y^2\right). \tag{158}$$

where σ_{bend} are normal stresses in the cross-section of the beam;

are tangent stresses in the cross-section of the beam; M_z is the bending moment in this cross-section; Q is the cross-cutting force; I_z is the inertia moment of the cross-section; y is the distant from the neutral sphere of the beam, and h - the thickness of the beam.

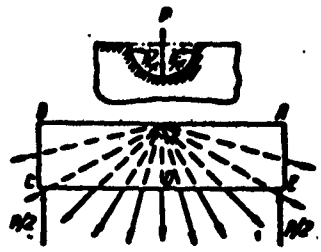

Fig. 40. Diagram of wedge action of force P in bending by concentrated force.

A more accurate investigation of the distribution of stresses in the beam on bending, taking into account the effect of local stresses appearing in the vicinity of points of load application /95, 99/ shows that the formula of resistance of material for maximum normal stresses (157) is correct also in this case; at the same time Formula (158) is very approximate and requires to be made more precise.

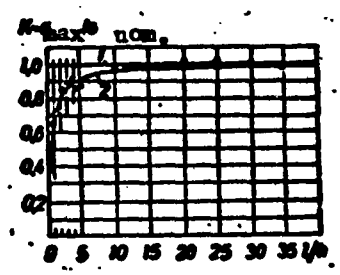

Fig. 41. Maximum elongation stresses in the center of the beam in bending by concentrated force:
1 - nominal stress σ_{nom}
2 - stress according to Formula (159).

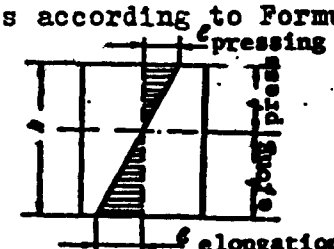

Fig. 42. Effect of difference of elasticity module of material in pressing and elongation on the distribution of stresses in cross-section of beam subjected to bending.

If we consider the wedge action of force P as shown in Fig. 40, stresses at point D can be presented in the form of

the following algebraic sum:

$$\sigma'_{\text{elong.}} = \frac{Pl}{4}\cdot\frac{6}{bh^2} + \frac{P}{nbh} - \frac{3P}{nbh} = \frac{Pl}{4}\cdot\frac{6}{bh^2}\left(1 - \frac{4}{3n}\cdot\frac{h}{l}\right). \tag{159}$$

where b is the width of the beam and l is the distance between resistances.

At high values of ratio h/l the effect of this factor can be very significant, as can be seen from Fig. 41. Dots on this curve indicate the experimental data obtained by M. Frokht /95/ and Koker and Faylon /100/ by the method of photoelasticity.

Formulas of resistance of materials /157, 158/ are not sufficiently accurate for the calculation of normal stresses in bending specimens made of materials which possess considerable differences in elasticity modules on elongation and bending.

These formulas can be made more accurate by the following method /101/.

Assuming the correctness of the hypothesis of flat cross-sections, we can write (Fig.42)

$$\frac{h_{\text{elong.}}}{h} = \frac{\varepsilon_{\text{elong.}}}{\varepsilon_{\text{press.}} + \varepsilon_{\text{elong.}}} \tag{160}$$

$$\frac{h_{\text{press.}}}{h} = \frac{\varepsilon_{\text{press.}}}{\varepsilon_{\text{press.}} + \varepsilon_{\text{elong.}}} \tag{161}$$

$$\varepsilon_x = ky. \tag{162}$$

For material with different elasticity modules on elongation and compressing, we will have

$$\frac{\sigma_{\text{elong.}}}{\varepsilon_{\text{elong.}}} = \frac{\sigma_{x\,\text{elong.}}}{\varepsilon_{x\,\text{elong.}}} = \frac{\sigma_{x\,\text{pr.}}}{\varepsilon_{x\,\text{pr.}}} \tag{163}$$

If we take into account Eq. (163), we will get

$$\sigma_{x\,\text{elong.}} = \frac{y\sigma_{\text{elong.}}}{h_{\text{elong.}}} = \frac{y\sigma_{\text{pr.}}}{h_{\text{pr.}}} \tag{164}$$

Then from equation

$$\int_{0}^{h_{elong.}} \sigma_{x\,elong.}\, b\,dy = \int_{0}^{h_{pr.}} \sigma_{x\,pr.}\, b\,dy \tag{165}$$

we will find

$$h_{elong.} e_{1.} h_{pr.} = h_{pr.} \tag{166}$$

and from equation

$$\int_{0}^{h_{elong.}} \sigma_{x\,el.}\, by\,dy + \int_{0}^{h_{pr.}} \sigma_{x\,pr.}\, by\,dy = M_{z} \tag{167}$$

we will get

$$\sigma_{el.} h^{2}_{el.} + \sigma_{el.} h_{el.} h_{pr.} = 3\frac{M_{z}}{b}. \tag{168}$$

or, taking into account (166)

$$\sigma_{el.} h^{2}_{el.} + \sigma_{el.} h^{2}_{el.} e_{pr.} = 3\frac{M_{z}}{b}. \tag{169}$$

Substituting into this formula the values of h_{elong} and h_{comp} from Eqs. (160) and (161), we will finally get

$$\sigma_{el.} = \frac{3M_{z}(\varepsilon_{el.} + \varepsilon_{pr.})}{bh^{2}\varepsilon_{el.}} = \frac{M_{z}}{W}\left(\frac{\varepsilon_{el.} + \varepsilon_{pr.}}{2\varepsilon_{el.}}\right); \tag{170}$$

$$\sigma_{pr.} = \frac{3M_{z}(\varepsilon_{el.} + \varepsilon_{pr.})}{bh^{2}\varepsilon_{pr.}} = \frac{M_{z}}{W}\left(\frac{\varepsilon_{el.} + \varepsilon_{pr.}}{2\varepsilon_{pr.}}\right). \tag{171}$$

Knowing the deformation of compressed and elongated filaments and using Formulas (170) and (171) we can estimate the error occurring in using the usual formulas of resistance of materials.

An estimate of the effect of this factor on the strength characteristic of metal-ceramic materials[1] on a base of SiC, Cr_3C_2 and TiC was made with pure bending using pick-offs of ohmic resistance according to the method described above, and it was found that the difference in the relative deformation of compressed and elongated filaments lies within the limits of the accuracy of measurement.

The results of these investigations are partially given in Fig. 35. In making specimens for bending tests by the powder

metallurgy method, one can encounter, as has already been noted, their deformation in the process of thermal processing, which can produce an error in tests.

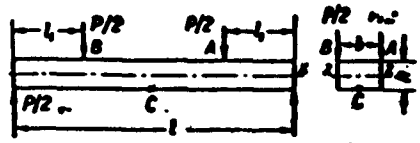

Fig. 43. Diagram of joint action of bending and twisting on specimen.

Thus, in applying loads according to the diagram shown in Fig. 43, in addition to bending stresses, we also get considerable twisting stresses.

In the extreme case the twisting moment will equal Pb/2. Timoshenko /99/ gives the following formula for the determination of maximum elongation stresses, produced in a rectangular beam, jointly with the action of twisting and bending moments (point C):

$$\bar{\sigma}_{el.} = \frac{M_z}{2W} + \frac{1}{2}\sqrt{\left(\frac{M_z}{W}\right)^2 + \left(\frac{2M_{tw}}{\alpha bh^2}\right)^2}. \qquad (172)$$

where M_{tw} is the twisting moment; α is the coefficient affected by the ratio b/h.

The error admissible in neglecting this factor, is determined by the formula

$$\frac{\bar{\sigma}_{el.} - \sigma_{el.}}{\sigma_{el.}} \cdot 100\% = \left(\frac{1}{6l_1}\sqrt{9l_1^2 + b^2/\alpha^2} - \frac{1}{2}\right) \cdot 100\%. \qquad (173)$$

Certain data derived according tc this formula are cited in Table 17.

Stresses appearing in a beam bent upwards with a radius of curvature R on pure bending, can be found according to Formula (101)

$$\sigma'''_{\text{elong.}} = \frac{6M_z}{bh^2}(1 - 0{,}25h/R). \qquad (174)$$

Table 17

b	h	l_1		$\frac{\sigma'''_{\text{elong}} - \sigma_{\text{elong}}}{\sigma_{\text{elong}}} \cdot 100\%$
1	1	1	0.208	45
2	2	2	0.246	34
1	1	2	0.208	13

The error caused by this factor can have an essential meaning only for considerable magnitudes of ratio h/R, which is excluded in practice.

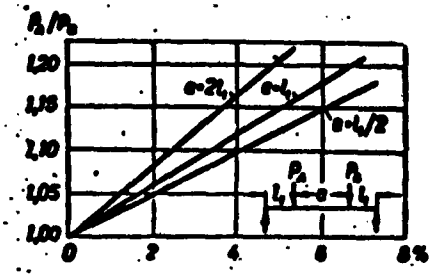

Fig. 44. Effect of unequal forces P_A and P_B on stresses in bending.

A certain amount of error in measuring stresses in tests by the diagram of pure bend can be produced by an inequality of forces applied to the specimen. In Fig. 44, on axis of the abscissae we have plotted the maximum error appearing from the assumption that $P_A = P_B$.

In works /53, 101/ during tests under conditions of pure

bending, a rectangular prismatic specimen with greater thickness along the edges (in places of contact) was used with resistance and loading prisms, which made it possible to avoid the effect of local stresses in the operational part of the specimen.

The latter has essential shortcomings, viz.: at the point of transition there can appear a considerable concentration of stresses, and making specimens of this shape is more complicated.

The effect of local stresses in the case of pure bending is insignificant, it does not increase elongation stresses, but on the contrary, reduces them, and their effect dampens at a very small distance from the area of application of force. For tests in bending by concentrated force, when the effect of local stresses is most significant, a specimen of this shape is inappropriate.

Testing of metalloceramic specimens for bending under normal and high temperature was conducted on a hydraulic press type "BLW" by means of an attachment specially designed for this purpose*), a sketch of which is given in Fig. 45.

Specimen 5 is placed on two prisms 11 made of high melting metalloceramic material, consisting of Cr_3C_2 and binder Ni. Prisms 11 together with resistors 3 can be moved along straight lines 1, which makes it possible to test specimens of different length.

*) The variant of the attachment for tests for bending as well as the attachment for tests for elongation cited before, were designed by V. M. Rudenko, Engineer.

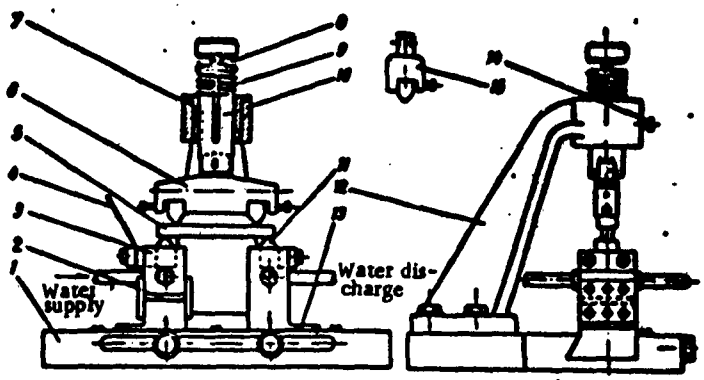

Fig. 45. Apparatus for bending tests at room and high temperature.

The load is applied to the specimen by means of special frames 6 and 15, hinged to plunger 10, through which the load is transmitted from the hydraulic press. Insertion of variable frames makes it possible to test specimens both by concentrated force bending, as well as pure bending.

The loading prisms are made of material on a base of silicon carbide which is highly heat resistant and a poor electrical and heat conductor.

Specimens are heated by passing electric current directly through them.

Measurement of temperature distribution along the length of the specimen by means of a thermocouple placed in a boring with an aperture of 2.5 mm (Fig.46) in the center of the specimen has shown that the temperature of the specimen within the range of its operational part remains practically unchanged.

Since specimens of regular geometric shape were selected for tests, the effect of deformation of the shape of specimens on strength was not taken into account.

In tests for bending by concentrated force, breakdown stresses were calculated taking into account local stresses, according to Formula (159).

Bending tests were conducted on prismatic specimens of rectangular cross-section. In investigating the effect of dimension on the strength characteristics, specimens were made in a majority of cases with adherence to the law of geometric similarity.

Thus, in testing specimens from material on a base of SiC, the following nominal operational dimensions of specimens were accepted: 1) 4.5 X 6 X 33.7 mm (V_{oper} = 911 mm^3); 2) 9 X 12 X 67.5 mm (V_{oper} = = 7290 mm^3); 3) 12 X 16 X 90 mm (V_{oper} = 17,280 mm^3); 4) 18 X 24 X 135mm (V_{oper} = 58,320 mm^3).

In the case of cermet on a base of Cr_3C_2 specimens used were: 1) 2.5 X 5 X 25 mm (V_{oper} = 312.5 mm^3); 2) 10 X 10 X 75 mm (V_{oper} = 7,500 mm^3); 3) 10 X 20 X 100 mm (V_{oper} = 20,000 mm^3).

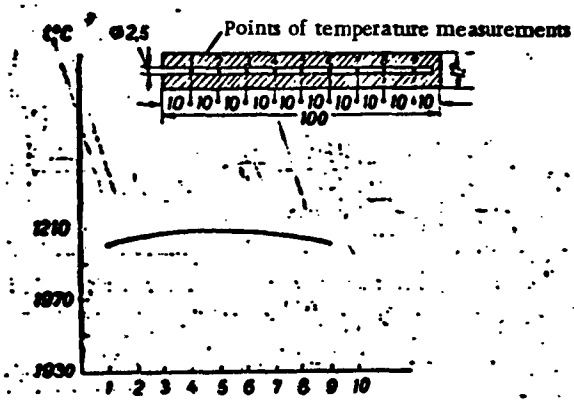

Fig. 46. Temperature distribution along the length of the specimen.

Specimen 2) of cermet on a base of Cr_3C_2 is geometrically unlike the other specimens.

Investigations of sensitivity of concentration of stresses were conducted in pure bending on specimens where a volume of 9 X 12 X 65.7 was subjected to pure bending.

The coefficient of sensitivity to concentration of stresses was determined according to formula

$$q = \frac{K_{ef} - 1}{K_T - 1}. \qquad (175)$$

where K_{ef} is the effective coefficient of concentration of stresses which is determined as the ratio of strength of the specimen without incision to the strength of an incised specimen; K_T is the theoretical coefficient of concentration of stresses calculated according to the formula of Neyber /102/. In our case $K_{ef} = 1.96$ and $K_T = 2.78$.

Correspondingly the radius of curvature q equalled 1.75 mm and 0.6 mm. In some cases (this also refers to specimens for elongation tests) the dimensions of specimens differed from the nominal, which was caused by engineering factors. Geometrical characteristics and volumes of specimens were not taken into account in calculations.

Twisting. The shape and dimensions of specimens tested for twisting are given in Fig. 47, and the diamgram of the apparatus in Fig. 48.

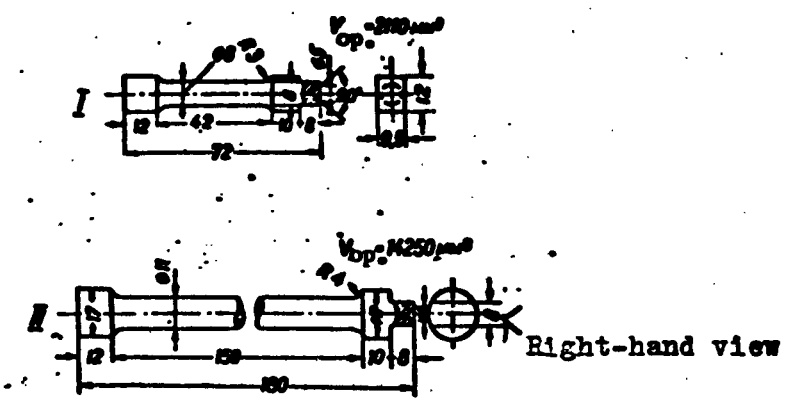

Fig. 47. Shape and dimensions of specimens for testing metalloceramic materials for twisting.

Specimen 1 is attached by the immobile lower end in vises 2 of base 3. The upper end of the specimen is attached in horizontal frame 4, which can turn on the immobile center 5.

Two cables 6 and 7 are attached to the frame, the cables passing over rollers 8 and 9 and joined to crossbar 10. The latter has platform 11 for loading.

For measuring the angle of twist of the specimen tested, an attachment is used, consisting of two mirrors 12 and 13, mounted on the specimens by means of yokes which, to avoid overheating, are cooled with water from two Martens tubes with scales. Using the well-known corelations for mirror systems, we can find the angle of twist of specimen over a certain length of the specimen under a given load.

The minimum twist angle which can be measured with the given apparatus constituted $1.25 \cdot 10^{-4}$ rad., which corresponds to the relative angle of twisting $8.4 \cdot 10^{-6}$ rad/cm for specimen type 1) (see Fig. 47).

The corresponding breakdown stresses can be found in the case of a linear dependence between the twisting moment and twist angle according to the well-known formulas of resistance of materials

$$\tau_{max} = \frac{M_{tw} d}{2 I_p}; \tag{176}$$

$$I_p = \frac{\pi d^4}{32}, \tag{177}$$

where M_{tw} is the twisting moment; I_p is the polar moment of inertia of the cross-section and d is the diameter of the specimen.

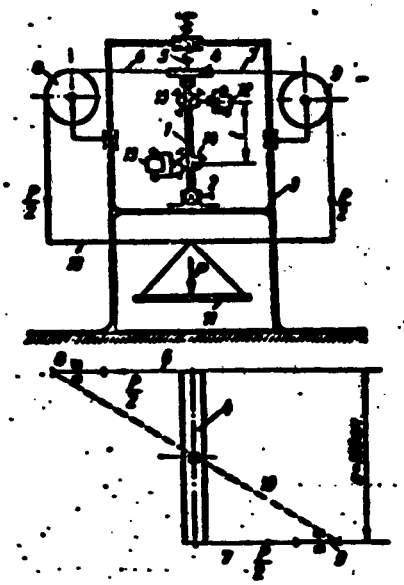

Fig. 48. Apparatus for twisting tests.

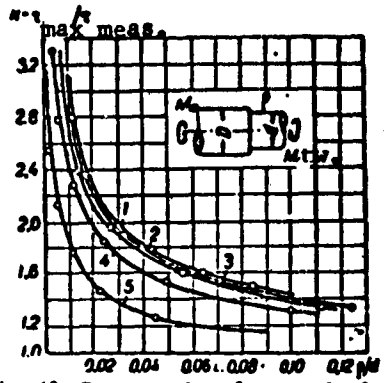

Fig. 49. Concentration of stresses in place of transition during twisting.

$1-\frac{D}{d}=2.00;\quad 2-\frac{D}{d}=1.50;\quad 3-\frac{D}{d}=1.33;$
$4-\frac{D}{d}=1.20;\quad 5-\frac{D}{d}=1.09.$ (82A)

In the absence of linear function the stresses can be found according to the Ludvik formula /57/

$$\tau_{max.}=\frac{4}{\pi d^3}\left(3M+\theta\frac{dM_{tw}}{d\theta}\right). \qquad (178)$$

where $\theta=\varphi/l_0$ is the twist angle per unit of length; $dM_{tw}/d\theta$ can be experimentally determined by the angle of incidence of curve $M-\theta$.

There are some difficulties in making specimens of relatively large dimensions with sufficient accuracy. However, it was found possible with materials under investigation.

The concentration of stresses in places of transition was insignificant for the given specimens, all specimens broke down in the operational part, and the breakdown occurred in areas of maximum elongation stresses, i.e., at an angle of 45° to the production area of the specimen.

Data on concentration of stresses during twisting of round specimens can be found in Fig. 49/ 103, 104/.

Investigations of some authors show /105, 106/ that the strength characteristics of metalloceramic materials are very strongly affected by the rate of load application /105, 106/, by the medium in which tests are conducted /106/ and others, and in this connection all conditions in the process of testing remained unchanged: rate of

load application in tests for elongation and bend were in the range of 10 → 20 kg/mm^{2}sec, and tests were made in regular atmosphere.

3. Results of Investigations and their Analysis

Figures 35 and 50 show the dependence between stress and deformation for investigated metal-ceramic materials on the base of chromium carbide, titanium and silicon carbide at room temperature, obtained with the help of ohmic resistance pick-offs according to results of tests of specimens under conditions of pure bending. These tests at room and high temperature (1250°) were made on metal-ceramic material on the base of SiC (Fig. 51) during twisting.

The results obtained show that the dependence between stress and deformation for all materials investigated remains practically linear both at room as well as high temperature.

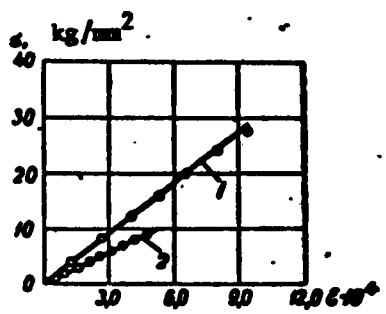

Fig.50. Dependence between stress and deformation for investigated materials: 1 - material on the base of TiC; 2 - materials on the base of SiC (composition 1).

Tests of these materials for twist, bend and elongation at room and high temperature did not provide a single instance of noticeable leftover deformation after the breakdown of specimens.

Results obtained in investigations of short-duration strength of these materials for twist, elongation and bend by concentrated force

and pure bend of smooth and incised specimens are given in Tables 18, 20 and 21.

Tests were conducted by methods and with specimens described above.

These tables, along with mean arithmetical values of the endurance limits also show temperatures under which tests were made, the operational volume of specimens, number of specimens tested to obtain a single experimental point, and lots of specimens *.

The limit of strength in elongation, twisting and pure bending was determined by the usual formulas of resistance of materials; in bending by concentrated force Formula (159) was used.

The results obtained in investigations of the effect of the dimensions of specimens on strength characteristics in beinding by concentrated force are given in Table 18, as well as in Figs. 52 and 53 in the form of curves in coordinates $\log \sigma$ - $\log V$.

The data obtained indicate that strength characteristics of the tested metaloceramic materials are very materially affected by the dimensions of the tested specimens. With an increase of sizes of specimens, the strength of all investigated materials essentially diminishes.

---

*) In some instances the engineering method of making metaloceramic[1] specimens differed somewhat from the method described above, but the composition of the material remained unchanged, which was associated with the research. In this connection, the results obtained in testing specimens from different lots were not compared.

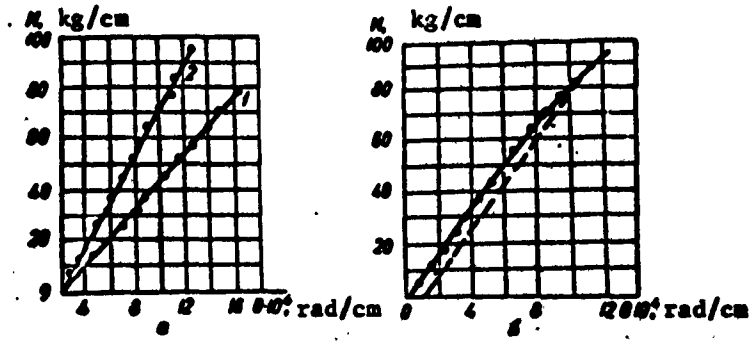

Fig. 51. Dependence between M and in twisting for material on the base of SiC: a - temperature 20°; 1 - composition 6; 2 - composition 3; b - temperature 1250°, composition 3.

A decrease of strength with an increase of size of specimens occurs both at room, as well as high temperature. Experimental points are placed on straight lines in logarithmic coordinates, therefore the dependence between the limit of strength and volume of specimens can be stated in the following form:

$$\lg \sigma = A + B \lg V. \tag{179}$$

i.e., it corresponds to the statistical theory of brittle strength of Wribull. Taking into account the designations accepted by Weibull, Formula (179) will be in the form

$$\lg \sigma = \lg [2^{1/m} (m+1)^{2/m} \sigma_0 I_m] - \frac{1}{m} \lg V. \tag{180}$$

Table 18

Material	Lot of Specimens	Operational volume of spec. mm^3	Temperature of test, °C	Number of tested spec.	Mean value of limit of strength kg/mm^2
On the basis of SIC Composition1	A	2470	20	15	12,0
			1200	15	14,80
		6420	20	25	10,00
			1200	15	11,80
" 2	B	935	20	8	14,50
			1200	7	15,20
		7400	20	8	11,30
			1200	10	12,20
		16100	20	10	10,60
		13700	1200	10	11,30
" 3	C	911	20	14	14,90
		7290	20	15	9,15
		17280	20	15	7,08
" 4	D	911	1200	25	14,30
		7290	1200	20	10,80
		17280	1200	15	9,30
		54500	1200	10	8,00
" 5	E	6900	20	10	6,00
		7290	20	13	5,45
		54500	20	10	4,35
" 6	F	911	20	30	7,08
		7290	20	25	5,40
		17280	20	10	4,80
		66610	20	10	3,96
Cermet* (85% Cr_3C_2; 15% Ni)	G	322,5	20	10	29,7
			950	10	26,5
		7500	20	10	20,7
			950	10	19,1
		20000	20	10	18,4
			950	10	16,6

* Result obtained by V.M. Rudenko, Engineer, Institute of Metaloceramics and Special Alloys, Academy of Sciences Ukrainian SSR

The magnitude of parameter m which takes into account the homogeneity of the material, can be determined from equation

$$\lg \sigma_1 - \lg \sigma_2 = \frac{1}{m}(\lg V_2 - \lg V_1). \qquad (181)$$

where σ_1 and σ_2 are limits of strength found in testing specimens of volumes V_1 and V_2, respectively.

Parameter σ_0 is found directly from Formula (100). Table 19 shows the values of parameter m for metal-ceramic materials on the base of SiC and Cr_3C_2 found according to Formula (181) for all possible combinations of σ_1 and σ_2.

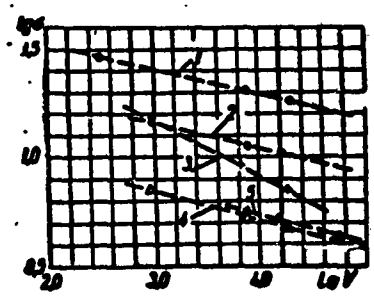

Fig. 52. Effect of dimensions of specimens on strength at room temperature: 1 - cermet on the base of Cr_3C_2; material on base of SiC; 2 - composition 2; 3 - composition 3; 4 - composition 6; 5 - composition 5.

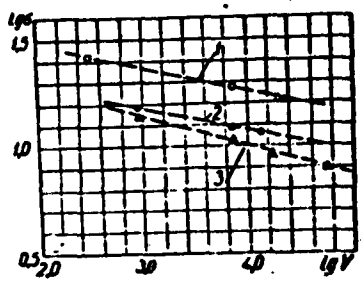

Fig. 53. Effect of dimensions of specimens on strength at high temperatures: 1 - cermet on base of Cr_3C_2 (950°); 2 - material on base of SiC, composition 2; 3 - composition 4 (1200°).

Magnitude σ_b was determined for every material and temperature according to the results of investigations of speciemens with a minimum volume, using mean value of parameter m_{mean}.

Table 19

Material	Temperature °C	m_{min} / m_{max}	m_{mean}	σ_0
On base of SiC:				
Composition 1	20	—	3,53	43,9
» 1	1200	—	4,21	40,28
» 2	20	8,29—12,14	9,84	17,65
» 2	1200	9,01÷9,07	9,04	19,04
» 3	20	3,36÷4,26	3,86	35,37
» 4	1200	6,00—7,37	6,90	18,00
» 5	20	5,90÷7,90	6,98	11,41
» 6	20	7,02—7,94	7,43	9,71
Cermet (85% Cr_3C_2; 15% Ni)	20	8,32÷8,71	8,55	33,60
	950	6,99÷9,61	8,47	29,90
Cermet (70% TiC)	20	—	4,09*	62,3*
Phosphorous steel [60]	—194	23,8÷25,4	24,5	62,3
Steatite [107]	20	—	19,2*	—
Low-carbon steel [108] (liquid limit)	20	—	56	61,5
Cermets of different composition [87]	20	—	6—15*	—
Modified corundum [46]	20	—	6,00*	65,3*
Rock salt [61]	20	—	3,10	4,46
Molybdenum silicide [97]	20	—	6,9*	—
Solid silicon carbide [27]	20	—	4,0*	—
	1480	—	3,0*	—
Graphite [27]	20	—	2,0—5,0*	—
	1480	—	2,3—4,0*	—
Modified cast iron (σ_{-1} = 22,4 kg/mm² provisional) [109]	20	—	6,48	171,4
Globular cast iron (σ_{-1} = 24,4 kg/mm² provisional) [109]	20	18÷8,97	9,1	183,0

* The values of m and σ_0 were found from the results of tests of one group of specimens of identical dimensions

ited in Table 19 are also the values of parameters m and σ_0 for other materials according to the investigations of different authors.

Strength characteristics of metal-ceramic materials on the base of Cr_3C_2, SiC and TiC found in tests for elongation, bend and twist, are given in Table 20.

The effect of uneven heating of specimens on strength in elongation tests was not taken into account, since the strength of these materials remains practically identical within the temperature range of 20 to 1200°.

The column "Theoretical value of strength" contains results obtained according to Formulas (98), (100), (102) and (103) with the use of parameters m_{mean} and σ_0 found according to the results of testing the same lots of material in bending by concentrated force.

If we rely on the widespread opinion that in the absence of plastic deformation breakdown should occur upon reaching critical values by maximum normal stresses, then in tests of brittle metal-ceramic materials for strength the coefficient of sensitivity to concentration of stresses, determined according to Formula (175), should be close to unity.

Table 20

Material	Specimen lot	Form of test	Operational vol. of specimens, mm^3	Temperature of tests, °C	No. of tested specimens	Experimental value of strength kg/mm^2	Theor. value of strength kg/mm^2	$\frac{\sigma - \sigma^*}{\sigma} \cdot 100\%$
On base of SiC Composition 1	A	Elongation	1730	20	15	4,40	4,13	6,9
		Pure bend	5630	1200	13	9,20	9,22	10,6
» 3	B	Elongation	1250	20	15	5,00	4,75	5,0
» 4	C	Elongation	1250	1200	13	6,60	5,26	10,3
		Twisting	14250	1200	8	5,70	5,26	7,7
» 6	D	Elongation	1250	20	10	3,30	3,03	8,9
		Twisting	2110	20	10	4,10	4,00	2,5
		Pure bend	7290	20	14	4,80	4,02	16
Cermet (85% Cr_3C_2; 15% Ni)	E	Elongation	1730	20	47	11,1	—	—
		Bend by conc. force	2100	20	10	23,1	—	—
Cermet (70% TiC)	F	Bend by conc. force	1430	20	22	30,9	—	—
		Pure bend	1180	20	21	28,0	—	—

Table 21

Indicator	Material on base of SiC (composition 1 at temperature in °C		
	20		1200
K_σ	1,96	2,78	1,96
K_ε	1,04	1,55	1,01
q	0,04	0,14	0,01
m	3,63	3,63	4,22
q_{calcul} $(\gamma=1)$	0,02	0,05	0,02

Results obtained in tests of metalloceramic materials on the base of SiC (Table21) show that, regardless of the brittleness of these materials, their sensitivity to concentration of stresses is insignificant.

This fact can be explained as follows. Application on a specimen of incisions of given dimensions predisposes a most probable location of its breakdown, since under an identical bending moment of stress, appearing in the place of incision, stress will be greater as a result of the lowering of the moment of resistance of the cross-section, as well as due to the presence of a concentration of stresses.

Nevertheless, in connection with the fact that the zone of maximum stresses is very small, the probability of a dangerous defect being located in this zone diminishes, and characteristics of strength of material should somewhat increase, which can lower the effect of the factors stated above.

Using Formula (98), we will have in this case

$$\sigma_i = \sigma\left(\frac{V_1}{V_i}\right)^{1/m} \frac{1}{K_\sigma}; \qquad V_i = \alpha V_0, \tag{182}$$

where σ_i is the strength of incised specimens; σ is the strength of smooth specimens; V_1 is the operational volume of a smooth specimen; V_i is the volume of material located in the place of incision; α is the coefficient of correction. Further we get

$$q_{calcul} = \frac{K_\sigma\left(\frac{V_1}{V_i}\right)^{1/m} - 1}{K_\sigma - 1}. \tag{183}$$

Comparisons of calculated and experimantal data from results of tests of 10-15 specimens are given in Table 21.

Results obtained in tests of metalloceramic materials on the base of SiC (Table21) show that, regardless of the brittleness of these materials, their sensitivity to concentration of stresses is insignificant.

This fact can be explained as follows. Application on a specimen of incisions of given dimensions predisposes a most probable location of its breakdown, since under an identical bending moment of stress, appearing in the place of incision, stress will be greater as a result of the lowering of the moment of resistance of the cross-section, as well as due to the presence of a concentration of stresses.

Nevertheless, in connection with the fact that the zone of maximum stresses is very small, the probability of a dangerous defect being located in this zone diminishes, and characteristics of strength of material should somewhat increase, which can lower the effect of the factors stated above.

Using Formula (98), we will have in this case

$$\sigma_i = \sigma\left(\frac{V_1}{V_i}\right)^{1/m} \frac{1}{K_\sigma}; \qquad V_i = \alpha V_0, \tag{182}$$

where σ_i is the strength of incised specimens; σ is the strength of smooth specimens; V_1 is the operational volume of a smooth specimen; V_i is the volume of material located in the place of incision; α is the coefficient of correction. Further we get

$$q_{calcul} = \frac{K_\sigma\left(\frac{V_1}{V_i}\right)^{1/m} - 1}{K_\sigma - 1}. \tag{183}$$

Comparisons of calculated and experimantal data from results of tests of 10-15 specimens are given in Table 21.

The low sensitivity to concentration of stresses of brittle materials is also observed by other researchers. For example, this was observed by Kuntze /2, 110/ who tested for strength incised specimens of pig iron for elongation. Nevertheless, he could not explain this fact in detail.

An essential effect of concentration of stresses on strength can be expected with these materials in the instance when the concentration of stresses is extremely great, which happens, for example, on contact of poorly processed surfaces (see Fig.32), or when high stresses are present in a large volume of material.

An essential effect of microdefects on the strength of brittle metalloceramic materials is also manifest in the fact that breakdown does not always occur in cross-section with maximum normal stresses.

This is evident from Fig. 54, which gives the results of tests of 47 specimens of type VI (see Fig. 29) made of cermet on a base of Cr_3C_2 in the coordinates: distance from center of specimen - relative number of specimens which break down along the given cross-section.

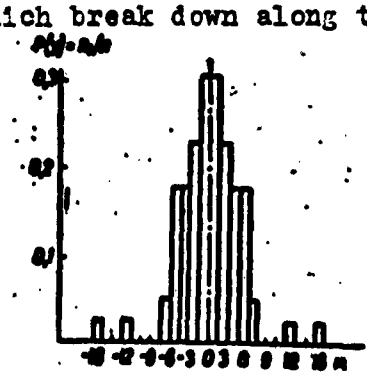

Fig. 54. Histogram of location of breakdown of metalloceramic specimens tested for elongation.

A very substantial effect on strength can be exerted by heterogeneity of material in the case of breakdown of parts under the effect of temperature changes (temperature impact).

The estimate of stability of material to temperature impact is very frequently determined in literature (for example /111/) according to the formula

$$A = \frac{k\sigma}{\alpha E}. \qquad (184)$$

where k is the coefficient of heat conductivity; σ is the strength of material for elongation; α is the coefficient of thermal expansion; E is the elasticity module of the material.

If we assume that for graphite A = 1, then for titanium carbide $A = 0.60 \cdot 10^{-2}$, for beryllium oxide $A = 2.1 \cdot 10^{-3}$, for magnesium oxide $A = 0.33 \cdot 10^{-3}$ /111/. The shortcoming of Formula (184) is that it does not take into account the effect of structural factors on the heat stibility of the part.

The effect of the dimension of a part on heat stability is usually calculated according to the Biot criterion formula

$$Bi = \frac{r_m h}{k}. \qquad (185)$$

where r_m is the distance along the normal from the axis or center plane of the part to the surface; h is the coefficient of heat transfer between the surrounding medium and surface; k is the coefficient of heat conductivity.

Nevertheless in the case of materials with a high degree of heterogeneity the effect of this factor can be more significant.

This can easily be shown on the example of determining the breaking down temperature differences for a plate which is heated to a temperature of t_0, and then cooled on one side by a coolant with a temperature of t_1.

Making use of the functions cited in the work of Kingery /112/ we can write

$$t_{max} = \frac{\sigma_{max}}{E\alpha(t_0 - t_1)}. \qquad (186)$$

where σ_{max} is the actual maximum stress at the surface of the plate; E is the elasticity module of the material; α is the coefficient of linear thermal expansion; t_0 is the initial temperature of the heated body; t_1 is the temperature of the cooling medium; σ'_{max} is the nondimensional stress.

Analyzing the ratios of breakdown temperature differences for two plates with a corelation of all dimension 1 : 2, we will find

$$M = \frac{(t_0 - t_1)_I}{(t_0 - t_1)_{II}} = \frac{\sigma'_{max\,II}}{\sigma'_{max\,I}} \cdot \frac{\sigma_{el\,I}}{\sigma_{el\,II}}. \qquad (187)$$

(index I refers to a plate of smaller dimensions, and II - greater dimensions).

Without taking the heterogeneity of material into account

$$M = \frac{(t_0 - t_1)_I}{(t_0 - t_1)_{II}} = \frac{\sigma'_{max\,II}}{\sigma'_{max\,I}} = \frac{Bi_{II}}{Bi_I} = \frac{r_{mII}}{r_{mI}} = 2 \qquad (188)$$

(on condition, naturally, that we assume the function of σ'_{max} and Bi in form (112)

$$\sigma'_{max} = Bi. \qquad (189)$$

If, however, we take into account the heterogeneity of material, which finds expression in the circumstance that the strength of parts of large dimensions will be lower, then function (187) will be in the form

$$M = \frac{(t_0 - t_1)_I}{(t_0 - t_1)_{II}} = \frac{r_{mII}}{r_{mI}} \cdot \left(\frac{V_{II}}{V_I}\right)^{1/m}. \qquad (190)$$

In the case of small values of parameter m, i.e., very heterogeneous materials, the magnitude of this ratio can be much greater; with m = 3 it will equal 4, with m = 6 it will equal 2.9 and so on.

Thus, with an increase of the dimensions of a part the breakdown temperature difference will decrease more substantially than it would

follow from Formula (185). This law was experimantally observed at the Institute of Metaloceramics and Special Alloys Acad Scien UkSSR during investigations of thermal stability of some heat resistant metaloceramic materials, which were considered above.

A detailed analysis of the effect of heterogeneity of material on stability to heat impact was given in the work of Manson and Smith /107/.

The values of parameters m and σ_0, which are part of the formula of Weibull's theory, can also be determined from the results of tests of one group of specimens of identical dimensions. According to this theory, the integral function of distribution of the strength of specimens is in the form (90)

$$P(\sigma) = 1 - e^{-\int_V n(\sigma)dV}. \qquad (92A)$$

The values of magnitude $B = \int_V n(\sigma)dV$ for different forms of state of stress were found earlier.

Taking these results into account, Formula (90) can be written in the following form:

$$P(\sigma) = 1 - e^{-\left(\frac{\sigma}{\sigma_0 A}\right)^m}. \qquad (92C)$$

Coefficient A depends on the form of the state of stress, dimensions of the specimen and parameter m. The value of this coefficient, depending on the form of the state of stress, is given in Table 22.

Table 22

Form of State of Stress	A
Elongation of specimen with uniform cross-section	$V^{-1/m}$
Elongation of specimen with cross-section changing according to the law $F_y = F_{min} + ay^2$	$[2A\delta_{min}^m l]^{-1/m}$
Bend by concentrated force of beam of rectangular cross-section	$\left[\frac{V}{2(m+1)^2}\right]^{-1/m}$

(table 22 continued)

Pure bend of beam of rectangular cross-section	$\left[\frac{V}{2m+3}\right]^{-1/m}$
Twisting of round rod	$\left[\frac{2V}{m+3}\right]^{-1/m}$

Taking these designations into account, the parameters of m and σ_0 can be found from Formulas (48), (56) and (57).

Results of such analysis for some metalloceramic materials on a base of chromium, titanium and silicon carbide are given in Figs. 55 and 56.

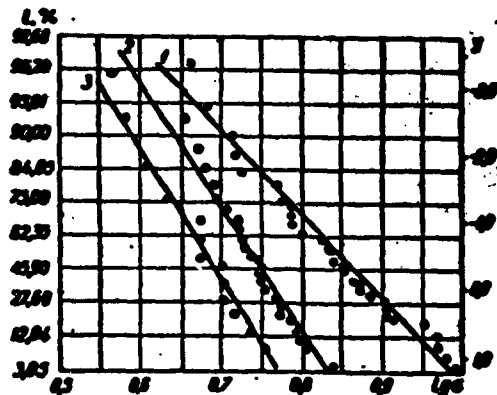

Fig. 55. Results of tests of metalloceramic material on a base of SiC (composition 6) in bending by concentrated force (20°) and at $m_{mean} = 7.06$, $\sigma_{0mean} = 10.20$ kg/mm^2.

The design of diagrams and plotting of experimental points on these Figures were made plotting paper according to the method described above (see Chapter two).

Data obtained from the analysis of the results of tests of composition 6 on a base of SiC indicate that parameters m and σ_0 have a certain dispersion, nevertheless their mean values are very close to the values cited in Table 19. For other investigated material no similar analysis was conducted due to the small quantity of identical specimens from one lot subjected to tests.

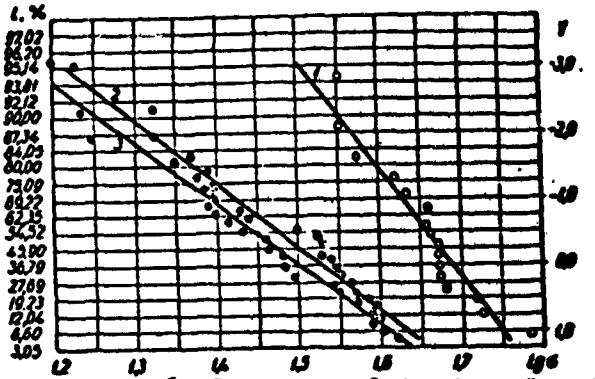

Fig. 56. Results of tests of metaloceramic materials (20°): • - material on base of TiC, pure bend; ⊕ - material on base of TiC, bend by concentrated force; ⊙ - material on base of Cr_3C_2, bend by concentrated force: 1 - V = 1310 mm^3, m = 7.20, σ_0 = 67.0 kg/mm^2; 2 - V = 1430 mm^3, m = 4.20, σ_0 = 74.03 kg/mm^2; 3 - V = 1180 mm^3, m = 3.98, σ_0 = 91.0 kg/mm^2.

As shown in Figs. 55 and 56, the law of distribution of strength of the investigated metaloceramic materials is close to the function expressed in Formula (48).

In estimating the strength of materials which possess a substantial dispersion of strength characteristics, it is important to know not only the mean value of strength and the effect of structural factors, but also the stress at which the probability of breakdown of the specimen or part will be insignificant (for example, 1% or 0.1% etc.). In order to be able to answer this question, we must know the law of distribution of strength and the parameters of this distribution. Then we can determine the probability of breakdown at a certain stress. An example of this was considered above (see Chapter two), for the case of normal distribution. Analogously this can be done in the case of distribution (48) and others.

In estimating the dispersion of strength characteristics it is convenient to have data indicating how many times it is necessary to reduce stress (in comparison with mean strength), so that the proba-

bility of breakdown would be insignificant.

In the case of distribution (48) the probability of no breakdown will have the form

$$l = e^{-\left(\frac{\sigma}{\sigma_0 A}\right)^m}$$

or

$$-\ln l = \left(\frac{\sigma}{\sigma_0 A}\right)^m; \tag{191}$$

$$\lg|-\ln l| = m \lg\left(\frac{\sigma}{\sigma_0 A}\right).$$

Designating

$$\frac{\lg|-\ln l|}{m} = d, \tag{192}$$

we will get the expression for stress, at which the probability of no breakdown will equal 1,

$$\sigma = 10^d \sigma_0 A, \tag{193}$$

then

$$t = \frac{\sigma^*}{\sigma} = \frac{l_n}{10^d}. \tag{194}$$

Magnitude t, which can be called the coefficient of safety, depends on parameter m and probability of no breakdown 1, and represents the ratio of mean stresses (σ^*) to stresses which correspond to a certain probability of no breakdown. The dependence of this magnitude on parameter m for $l_1 = 0.99$ and $l_2 = 0.999$ is given in Fig. 57.

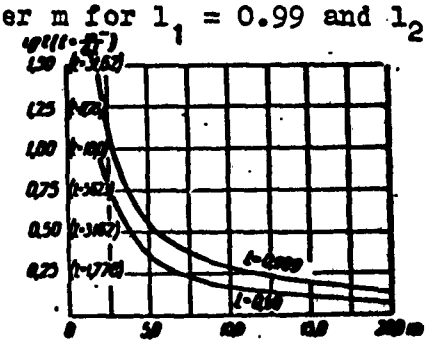

Fig. 57. Dependence of the coefficient of safety on the coefficient of homogeneity m.

These data indicate that the coefficient of safety substantially increases at $m < 5 - 7.5$.

Using the above formulas, we can find the stress, at which there will be a certain probability of breakdown (1 or 0.1% etc.)

taking into account the dimensions and form of load of the specimen or part.

In a majority of investigated heat resistant metal-ceramic[1] materials the value of this parameter exceeds 5 - 7.5 and is close to the values of this maginitude for modified and globular pig iron (see Table 19), i.e., materials, which have a wide application in machine building.

Tests of a small number of specimens (20 to 30) does not make it possible to determine with reliability the form of function of distribution of general combination from which a given selection was made.

This is confirmed by results cited in Figs. 55, 56, 58-60, where identical experimental results are plotted on different plotting papers.

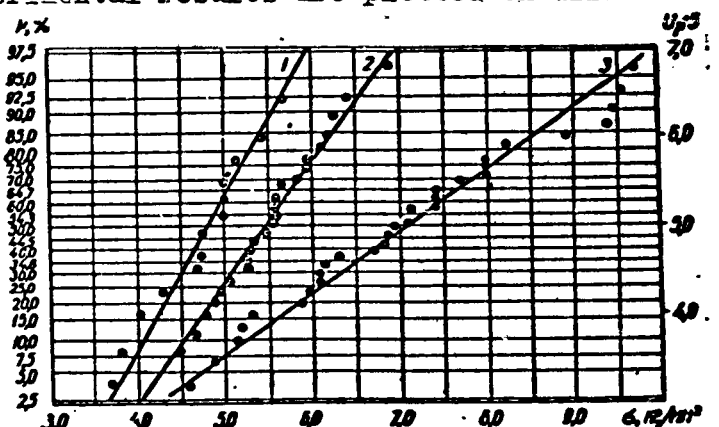

Fig. 58. Results of tests of metal-ceramic[1] material on base of SiC (composition 6) in bending by concentrated force: 1-V = 17280 mm^3, σ = 4.81 kg/mm^2, S^* = 0.56 kg/mm^2; 2 - V = 7290 mm^3, σ = 5.40 kg/mm^2; 3 - V = 911 mm^3, σ = 7.08 kg/mm^2, S^* = 1.44 kg/mm^2.

The first two curves are drawn on plotting paper which corresponds to the law $1 - e^{-ey}$, and the three others on plotting paper which corresponds to normal distribution.

In all these cases the points lie very close to straight lines corresponding to these distributions. For the purpose of detailed inve-

stigation of the function of strength distribution tests were made for bend of 189 identical specimens of metal[1]oceramic material on a base of Cr_3C_2 ($V = 1{,}000\ m^3$).

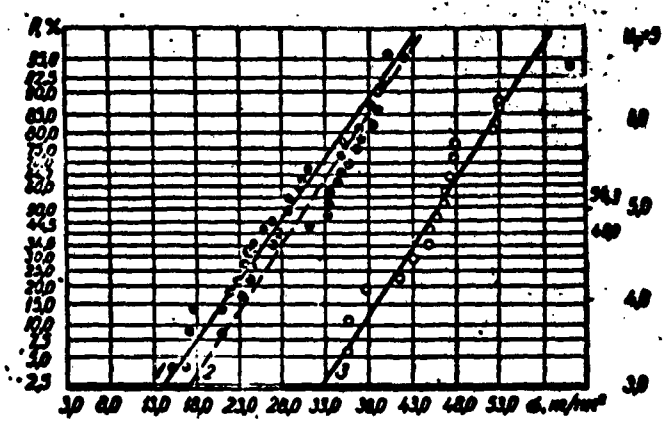

Fig.59. Results of tests of metal[1]oceramic materials (20°):
● - material on base of TiC, pure bend; ◉ - material on base of TiC, bend by concentrated force; ⊙ - material on base of Cr_3C_2, bend by concentrated force: 1 - $V = 1180\ mm^3$, $\sigma = 28.7\ kg/mm^2$, $S^* = 7.23\ kg/mm^2$; 2 - $V = 1430\ mm^3$, $\sigma = 30.8\ kg/mm^2$, $S^* = 6.87\ kg/mm^2$; 3 - $V = 1310\ mm^3$, $\sigma = 45.9\ kg/mm^2$, $S^* = 6.5\ kg/mm^2$.

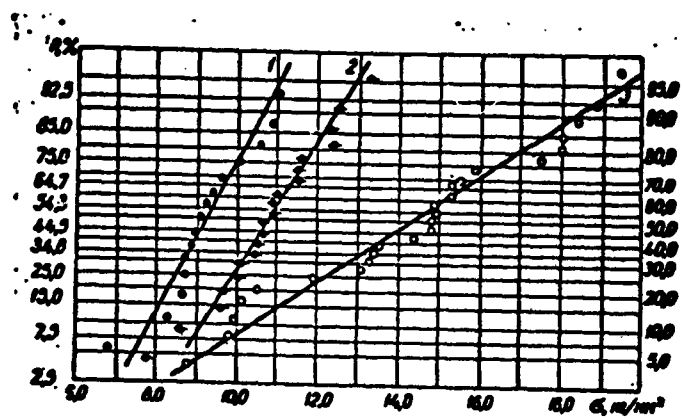

Fig. 60. Results of tests of metal[1]oceramic material on base of SiC (composition 4), bend by concentrated force (1200°):
1 - $V = 17280\ mm^3$, $\sigma = 9.30\ kg/mm^2$, $S^* = 1.13\ kg/mm^2$;
2 - $V = 7290\ mm^3$, $\sigma = 10.80\ kg/mm^2$, $S^* = 1.39\ kg/mm^2$;
3 - $V = 911\ mm^3$, $\sigma = 14.30\ kg/mm^2$, $S^* = 3.08\ kg/mm^2$.

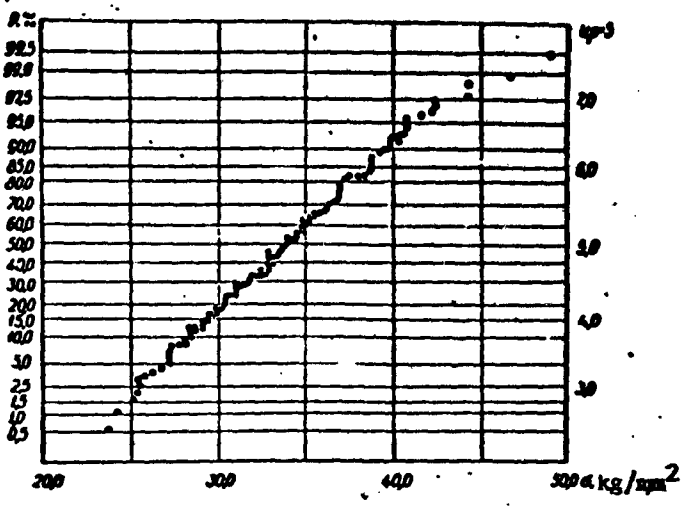

Fig. 61. Test results plotted on normal probability paper (85% Cr_3C_2 and 15% N.)
$\bar{\sigma}$ =34.0 kg/mm^2 $S^*(\sigma)$ = 4.41 kg/mm^2

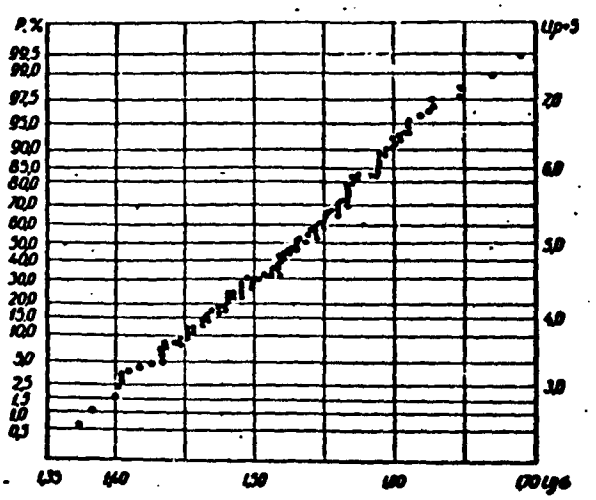

Fig. 62. Test results plotted on logarithmic normal probability paper (85% Cr_3C_2 and 15% Ni)
$\bar{\lg\sigma}$ = 1,527, $S^*(\lg\sigma)$ = 0,0568

The results obtained were plotted on probability papers, corresponding to four different distributions; normal distribution (Fig. 61), logarithmic normal distribution (Fig. 62); a distribution in the form of (Fig. 63), and distribution (195) in the form of

$$P(\sigma) = e^{-\left(\frac{\sigma}{K}\right)^{-n}}, \qquad (195)$$

which can be expressed by means of simple transformation in the form (55) (Fig.64).

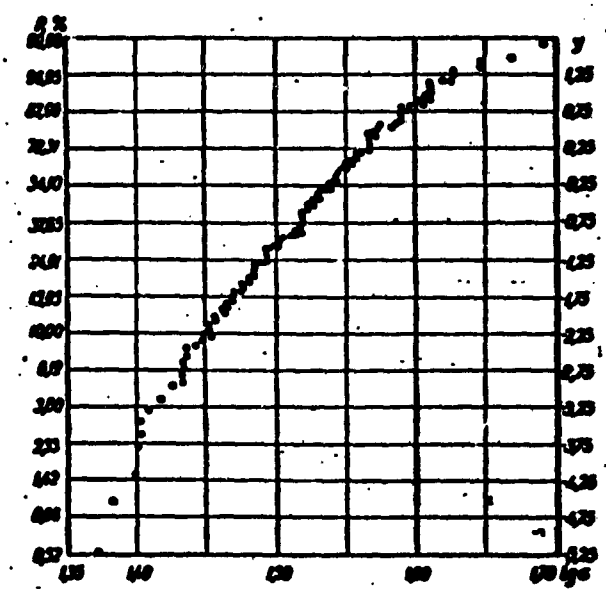

Fig. 63. Results of tests of specimens (85% Cr_3C_2 and 15% Ni), plotted on plotting paper, corresponding to distribution $P = 1 - e^{e^y}$, n = 9.42, K = 35.75

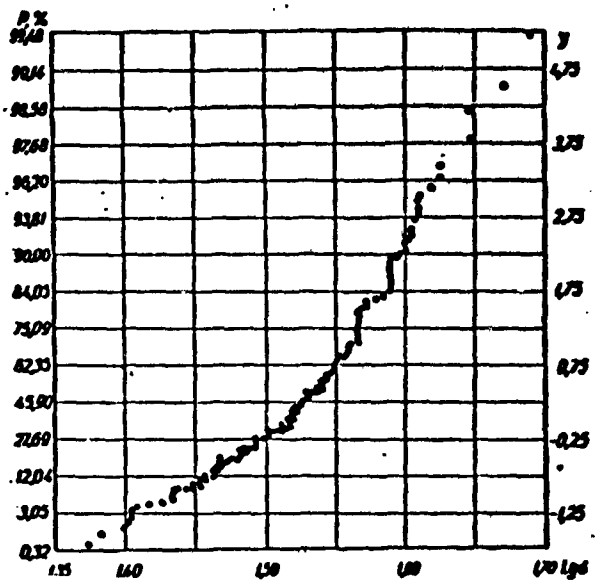

Fig. 64. Results of tests of specimens (85% Cr_3C_2 and 15% Ni) plotted on plotting paper, corresponding to distribution $P = e^{-e^{-y}}$, $n = 9.42$, $K_0 = 31.71$.

These diamgrams also show the values of the parameters of these distributions, found from experimental data. The paramaters of normal distribution ($\bar{\sigma}$; S^*) can be found from Formulas (19) and (22), in the case of logarithmic normal law, the parameters of distribution ($\log \bar{\sigma}$ and $S^*(\log \sigma)$ are determined by Formulas (59) and (58), in the case of distribution according to the law $\left[1 - e^{-\left(\frac{\sigma}{K}\right)^n}\right]$

the constants (m and K) can be found from Formulas (56) and (57), in the case of law $(e^{-\left(\frac{\sigma}{K}\right)^{-m}})$ the constant m is determined from Formula (56), and K_0 from formula

$$\lg K_0 = \lg \bar{\sigma} - \frac{y_0}{2{,}30259m}. \qquad (196)$$

where the same designations have been adopted as in Formula (57).

The criterion of correspondence of the experimental data to the distributions indicated above can be the proximity of the experimental points in these diagrams to straight lines.

As can be seen from Figs. 61-64, the best correspondence of the experimental data to the above distribution exists for the logarithmic normal law.

Table 23.

Type of distribution	Probability $P(\sigma)$ at $\sigma_1 = 16$ kg/mm^2	$\sigma_2 = 20$ kg/mm^2	$\sigma_3 = 26$ kg/mm^2
According to experimental data	0	0	0.0317
Normal	0.00023	0.008	0.0351
Logarithmic normal	close to 0	0.0001	0.0239
Form $P(\sigma)=1-e^{-\left(\frac{\sigma}{K}\right)^m}$	0.0005	0.0064	0.0485
Form $P(\sigma)=e^{-\left(\frac{\sigma}{K}\right)^{-m}}$...	close to 0	$2.81 \cdot 10^{-34}$	0.0015

Curves of these distributions are shown in Fig. 65 in the form of close probability, plotted by using previously found constants, and experimantal data are plotted in the form of a distribution polygon.

These results (Table 23 and Fig.65) show that distribution of type (48) at low stresses gives a somewhat greater probability of breakdown than other distributions, which indicates that the error permissible in this case, cannot cause a decreases of permissible stresses.

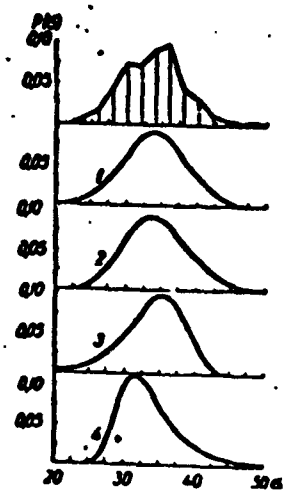

Fig. 65. Comparison of different forms of distribution, construed after experimental data.

$$1 - P(\sigma) = \frac{1}{\sqrt{2\pi}\,S_\sigma} e^{\frac{(\sigma-\bar{\sigma})^2}{2S_\sigma^2}};$$

$$2 - P(\lg\sigma) = \frac{1}{\sqrt{2\pi}\,S_{\lg\sigma}\sigma} \times e^{-\frac{(\lg\sigma-\lg\bar{\sigma})^2}{2S_{\lg\sigma}^2}};\quad 3 - P(\sigma) = \frac{m}{\bar{\sigma}_0^m}\sigma^{m-1} e^{-\left(\frac{\sigma}{\bar{\sigma}_0}\right)^m};\quad 4 - P(\sigma) = \frac{m}{\bar{\sigma}_0^m}\sigma^{-(m+1)} e^{-\left(\frac{\sigma}{\bar{\sigma}_0}\right)^{-m}}. \qquad (100A)$$

The following conclusions can be made on the basis of the results obtained.

The structural strength of products made from brittle metal-ceramic materials is very substantially affected by the dimensions of the parts, form of load, dispersion of strength characteristics, etc.

These laws are based on the substantial effect on the strength of similar materials of microdefects, fortuitously distributed over the volume of the material.

The effect of these factors on strength can be taken into account by means of using the statistical theories of strength, and of the Weibull theory in particular.

Using the formulas of this theory and relying on the results of tests of specimens, one can estimate the mean value of strength of a part of any dimension, taking into account the form of load and the presence of stress concentrators, also, which is particularly important, one should determine the probability of breakdown of this part at certain values of stress σ.

The constant of the material, necessary to use the formulas of the Weibull theory should be determined from the results of tests of large lots of specimens. This is particularly important in connection

with the fact that to this day there is no available method of determining the reliability of estimating these constants.

The Weibull theory does not correspond to experimantal data in all cases, it was found in particular that the logarithmic normal law of distribution of strength of specimens better corresponds to the results of tests of certain metaloceramic materials than the Weibull distribution.

The problem of devising reliable methods of calculating the strength of parts made from brittle metaloceramic materials makes it necessary to further develop the existing statistical theories of strength with respect to these materials, taking into account the specifics of their application (high operating temperature, rapid temperature changes, etc.).

Conclusions

1. The development of many branches of new engineering makes it imperative to devise new construction materials with a high melting temperature, high heat resistance and oxidation resistance, and other special properties. These materials and products from them, can be produced by the powder metallurgy method in a number of cases, using such compositions as oxides, carbides, silicides, nitrides, etc., which are brittle materials.

2. Investigations show that breakdowns of these materials are accompanied by phenomena which do not appear, or appear in very insignificant degree in the case of such widespread modern materials as steel and other alloys.

These laws include the substantial dispersion of strength characteristics, decrease of mean strength with the increase of the dimensions of parts, the effect of the form of load on strength characteristics (elongation, bend, pure bend, etc.).

In a whole series of cases the effect of these factors on strength is very substantial, which makes it necessary to devise reliable methods which will make it possible to estimate their effect on the strength of actual parts.

3. The nature of these laws is associated with the absence of plasticity in these materials and with the substantial effect on strength of various microdefects (pores, micro-cracks, impurities, etc.), in the proximity of which we can encounter substantial concentrations of stresses. In developing the formulas of the theory of elasticity and resistance of materials, and particularly in devising the theory of strength, no account is taken of the heterogeneous properties of individual microvolumes of actual materials, and in this connection these formulas cannot be used in calculating the strength of parts made of brittle metal[1]oceramic materials.

The effect on strength of fortuitously distributed microdefects in the volume can be calculated by developing statistical theories of strength.

4. The laws observed during breakdowns of brittle metal[1]oceramic materials (dispersion of results of tests, lowering of strength limit with increase of dimensions of parts, effect of form of load on strength characteristics, form of breakdown, especially in tests for compression, insignificant effect on strength of main stresses σ_2 and σ_3 etc.) find an explanation, if we take into account the heterogeneity of the properties if actual materials and the fortuitous character of the distribution of microdefects over the volume of the material.

5. A detailed investigation of the laws governing the breakdown of a number of metal[1]oceramic materials on a base of silicon carbide and chromium carbide has shown that the laws governing the breakdown of these materials have a statistical nature, and that the effect on strength of the dimensions, form of load, etc. can be calculated by

using the formulas of the Weibull statistical theory of brittle strength.

The advantages of this theory lie in its simplicity, small number of experimentally determined constants (m and σ_0), as well as in the opportunity to use these constants and estimate the effect on strength both of the structural factors, as well as dispersion of strength characteristics, which is of great practical importance. Investigations have also shown that with identical engineering methods of production of different specimens, the heterogeneity of material, which is characterized by the form of distribution of critical stresses in microdefects, remains approximately identical and can serve as a characteristic of brittle metal[1]oceramic materials. It was found that not all experimental data correspond to the formulas of the Weibull theory. This primarily refers to the law of distribution of the strength of specimens assumed by Weibull. Further theoretical research in this direction is therefore necessary.

6. Concrete data have been obtained from investigated metal[1]oceramic materials which indicate in particular that the homogeneity of the investigated materials, which is designated by the coefficient of homogeneity of material after Weibull as m, is mostly close to this magnitude for modified and globular cast iron, which is widely used as structural material in machine building.

7. The successful introduction of heat resistant metal[1]oceramic materials into engineering will be possible only in the event that, along with a further improvement of their properties and engineering methods of their production, special attention will be paid to devise reliable methods of calculation of the strength of parts; also to construction of parts, components of structures and whole structures, in which account would be taken of the peculiarities of deformation and breakdown of such materials.

DISTRIBUTION LIST

DEPARTMENT OF DEFENSE	Nr. Copies
HEADQUARTERS USAF	
AFCIN-3D2	1
ARL (ARB)	1
OTHER AGENCIES	
CIA	1
NSA	6
DIA	9
AID	2
OTS	2
AEC	2
PWS	1
NASA	1
ARMY (FSTC)	3
NAVY	3
NAFEC	1
RAND	1
AFCRL (CRXLR)	1

MAJOR AIR COMMANDS	Nr. Copies
AFSC	
SCFDD	1
DDC	25
TDBTL	5
TDBDP	5
AEDC (AEY)	1
AFSWC (SWF)	1
ASD (ASYIM)	1
ESD (ESY)	1